2009-01-01

Impacting Testing Of High Temperature Ceramics Through The Use Of A Vitiated Heater For Hot And Cold Fire Collisions

Adrian Trejo
University of Texas at El Paso, atrejo2@miners.utep.edu

IMPACTING TESTING OF HIGH TEMPERATURE CERAMICS THROUGH THE USE OF A VITIATED HEATER FOR HOT AND COLD FIRE COLLISIONS

ADRIAN TREJO

Department of Mechanical Engineering

APPROVED:

Jack F. Chessa, Ph.D., Chair

Arturo Bronson, Ph.D.

Cesar Carrasco, Ph.D.

Patricia D. Witherspoon, Ph.D.
Dean of the Graduate School

Dedication

This thesis is dedicated to my entire family for their past, present, and future support.

IMPACTING TESTING OF HIGH TEMPERATURE CERAMICS THROUGH THE USE OF A VITIATED HEATER FOR HOT AND COLD FIRE COLLISIONS

by

ADRIAN TREJO, B.S. Mechanical Engineering

THESIS

Presented to the Faculty of the Graduate School of

The University of Texas at El Paso

in Partial Fulfillment

of the Requirements

for the Degree of

MASTER OF SCIENCE

Department of Mechanical Engineering

THE UNIVERSITY OF TEXAS AT EL PASO

December 2009

Acknowledgements

I would first like to acknowledge Dr. Ahsan Choudhuri and all the employees from the Combustion and Propulsion Research Laboratory. These employees include but are not limited to Bidhan Dam, Carlos Gomez, Chance Garcia, Jesus Flores, and Vishwanath Ardha for sharing their knowledge and being present throughout many experiments to assure our safety. At the initial stages of this experiment many hands were needed and many students from the Combustion and Propulsion Research Laboratory kindly gave their assistance with enthusiasm. I would also like to acknowledge Arturo Acosta as he worked as a co-researcher throughout the entire project.

I would like to give my thanks to Dr. Arturo Bronson and Dr. Cesar Carrasco for taking their busy schedules and participating in my graduate committee. Dr. Bronson also offered his guidance which proved important in completing this project. Lastly, I would like to acknowledge my advisor Dr. Jack Chessa for giving me the opportunity to research and work as one of his graduate students. His vast knowledge in multiple areas also served as an important key in completing this research project.

Abstract

Material testing is a crucial step during the design process as particular materials serve as safety and life saving conditions. In this study, a $MoSi_2$ is chosen as the target specimen to undergo impact under high temperatures. An impact apparatus is designed and constructed for the purpose of propelling alumina particles at high velocities. A nozzle using compressed nitrogen gas is used to fire the particle at the desired velocities. Due to the possibility of thermal shock occurring at higher temperatures, a separate nozzle utilizing vitiation heating is designed to fire the particle at equally higher temperatures to prove the lack of thermal shock. Throughout the experiment, measurements including particle velocity, exit temperature, specimen temperature, and damage of the specimen are documented in both the cold test nozzle and vitiated heating test nozzle. Ultimately, the design of the impact apparatus is such that it may used as a characterization tool. Although the final results focus on the characterization of the $MoSi_2$ specimen and the damage associated, the impact apparatus may be used to characterize materials at any temperature application and is not limited to characterizing ceramics.

Table of Contents

List of Tables

List of Figures

Chapter 1: Introduction

1.1 Project Objectives

The experiment performed contains several objectives. The main objective is to build an apparatus capable of impacting a ceramic at high temperatures to indent, crack, or possibly fracture the material. The damage is then further investigated under a microscope. Other objectives necessary to achieve this goal are to design and construct two types of test nozzles. A Cold Fire Test Nozzle (CFTN) is designed for the purpose of only impacting the specimen assuming the absence of thermal shock. This nozzle fires the particle with an inert gas at room temperature. The second nozzle is a Vitiated Heating Test Nozzle (VHTN). The VHTN utilizes a vitiated heater to heat the exit flow as the particle is fired out of the nozzle. The purpose of this nozzle is to prevent any thermal shock that may occur. While the VHTN is preferred due to the fact it will minimize any possible thermal shock effects, the complexity is considerably more than the CFTN. Each nozzle must be designed to propel the particle while incorporating the particle parameters as shown in Figure 1.1. Another objective is to design and construct a stand that mounts each nozzle and incorporates the specimen being tested. Other equipment used will be designed such that the stand and nozzle remain stationary other than for the purpose of adjusting the nozzle towards the targeted specimen. In order to attain a better understanding of the final results, all the characteristics of each nozzle including the particle velocity, chamber pressures and exit temperatures must be measured. . All experiments and tests are performed in the Combustion and Propulsion Research Laboratory at The University of Texas at El Paso.

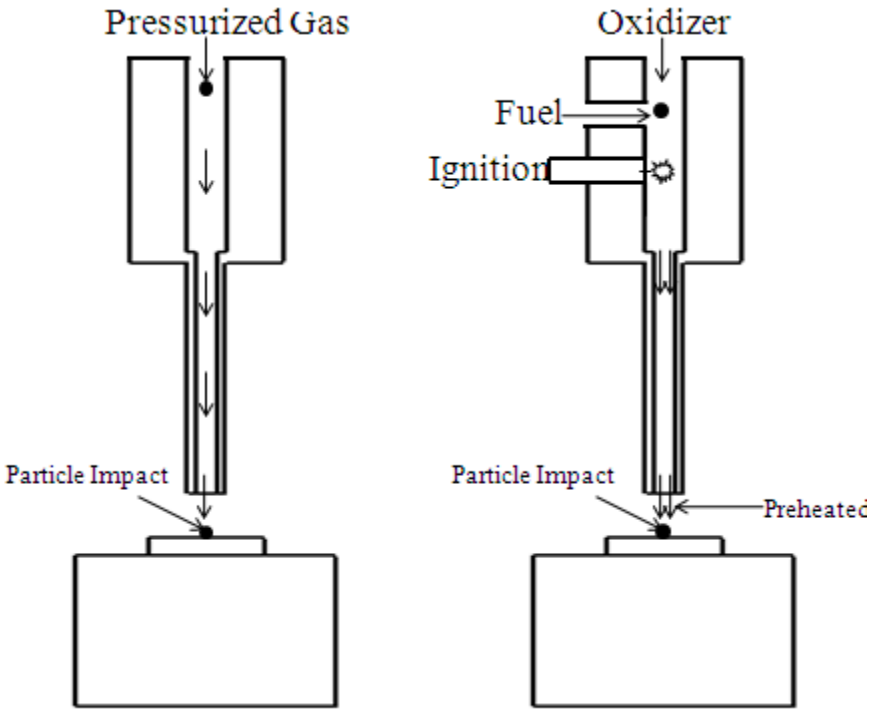

Figure 1.1: Illustration of the CFTN and VHTN Tests

1.2 Project Overview

Impact testing in many industrial applications serves as one of the most important tests a part designer must take into consideration. Enduring impacts serves as a critical condition in many applications as a part withstanding certain impacts serves as a life saving condition. Not only does impact testing determine whether or not a material is sufficient for certain applications, impact testing determines the properties of that particular material. In addition, material properties change under different environmental conditions in which the material is applied. In these circumstances, determining a material's properties is crucial under a wide variety of conditions. There are several types of impact tests which are a popular use for finding the ductility of materials. These tests are used in many industrial applications including aircraft industries, law enforcement, and automobile industries to name a few.

Impact testing requires another object to be propelled either by gravity and/or an external force

to make contact on the sample undergoing the impact. It is beneficial that the specimen is accurately impacted in the same location of the specimen. Furthermore, tests must be run to determine the dynamics of the particle upon exiting the nozzle. Initial tests also include the assurance of a collision each time the object is propelled at the determined velocity. Attaining proper accuracy means each nozzle must be aimed carefully while the specimen is in the proper position.

1.3 Parameters

1.3.1 Impact Apparatus Parameters

The addition of higher temperatures also increases the difficulty to operate standard material testing equipment as high temperatures cause a danger hazard and in many cases the equipment itself is not meant to withstand high temperatures. The impact apparatus must not fail from the heat radiating from the specimen or the heat created as the gases from the vitiated heater are ignited. The entire assembly of the impact is also designed to mount the CFTN and VHTN securely while small adjustments must be allowed for proper aiming of each nozzle. These adjustments include movements in the horizontal and vertical directions. It is also the intent of the impact apparatus to act as a rigid stand to incorporate measurement equipment and/or gas lines in either the CFTN of VHTN.

1.3.2 Particle Parameters

The parameters of the particle are defined by the weight, size, and velocity as it impacts the specimen. It is important to keep the size and weight of the particle fairly consistent throughout each experiment. Since the velocity calibration of each nozzle is performed separately from the impact test, the particle characteristics must be replicated in each test in order to achieve similar velocities. The particles used must also achieve velocities of up to 80-100 m/s or velocities sufficient enough to cause

damage to the specimen. The particle size and shape are spherical alumina particles with diameters between 2.05-2.20 mm and between .017-.019 grams.

Chapter 2: Literature Review

2.1 The Use of Ceramic Materials

Many research papers have studied ceramics under high temperatures due to the applications in which they are used. Ceramics have been most notably used in aerospace and nuclear industries as they are applied as thermal protectors under extreme heat experienced by space shuttles upon re-entry into the atmosphere, or exposure to nuclear waste [11]. Ceramics are used in a wider variety of applications however. Many types of ceramics such as alumina (Al_2O_3) and Silicon Carbide (SiC_2) have been used as bearings for their "combinations of chemical and mechanical properties" under friction conditions [5]. Ceramics have also been widely used as bone implants in the biomedical field as ceramics are biocompatible with a wear resistance that compares to a human bone [12].

In this research, a variety of ceramics were studied. It is important to investigate many ceramics and their particular applications in which they are applied. The particular ceramics in this paper were investigated for their structural integrity under high temperatures and electro physical properties. Ceramics such as alumina are primarily used for insulation considering their high electrical resistance and porous nature [11]. Mullite is a ceramic composite formulated from Al_2O_3 and Silica (SiO_2) taking after Al_2O_3 with a high electrical resistance [13]. $MoSi_2$ is used throughout industry as heating elements in furnaces and has been implemented as early as the mid 1960's by the High-Temperature Heating-Element Factory in Kirovakan, Armenia [7]. $MoSi_2$ composites have also been designed for higher flexural tests as presented in a paper by Tantra and Ramasesha by combining the effects of $MoSi_2$, titanium diboride (TiB_2), and SiC_2 [8].

2.2 Impact Testing

As many materials are implemented, proper material tests are essential depending on the type of research explored. An impact test is primarily to find the toughness characteristics of the material. Since

essentially the material test performed in this experiment is an impact test, current impact tests practiced were researched. Two notable impact tests are the Charpy and Izod tests. Each test employs a pendulum dropped from a known height in which the impact energy is calculated from the difference of initial and final potential energies [15]. Many situations call for the need to design and build an impact system from scratch. In the case of Belingardi and Vadori, a dart impact test experiment is designed to impact composite materials at low velocities through the use of gravity implementing the same principles of calculating the impact energy through the use of potential energy differences [6].

2.3 Vitiation Heaters and Combustion

Most vitiated heaters are implemented in air-breathing engines and air-breathing rockets contained in a number of test facilities [4]. Since air-breathing engines must maintain a certain inlet pressure and temperature, a vitiated heater acts as a preheat phase upon entering the engine. The use of vitiated heating involves an ignition between two gases, a fuel and an oxidizer, passing through a nozzle which increases the temperature as well as the pressure. The main flaw in vitiated heating is the ability to reach a stable flame. In a paper by Hashimoto, a vitiated-air heater is implemented on coaxial injectors to maintain a Hydrogen (H_2) and oxygen (O_2) flame [4]. The experiments in this paper proved successful with stable pressures and temperatures of up to 6.0 MPa and 1400K respectively was achieved. Another paper presented by Pitani discusses the problems of ignition within the chamber of the vitiated heater employed on a supersonic combustion ramjet (scramjet). In this experiment, ignition times of various gas combinations in a vitiated-air heater are studied. It is concluded that the problem of premature ignition was due to contamination containing residual radicals affected the delay time of ignition. Although premature ignitions existed in gases resulting in H_2O, the paper still suggests that vitiated heaters are a more reliable way of reaching high air temperatures as opposed to arc heaters and ceramic storage heaters [3].

In this experiment, the vitiated heater will not be designed to work in an engine but too function

as a preheating system. Combustion properties of various chemicals such as hydrogen and methane have been extensively researched. Ignition time was researched by Bubnovich for various excess air coefficients. This paper also discusses the ignition temperatures needed in order to achieve the phenomena of combustion. In 1981, Warnatz tested ignition limits in hydrocarbon-air mixtures as well as hydrogen-oxygen mixtures 1981. These tests discovered, through a pressure and temperature diagram, that explosion limits exist as illustrated in Figure: 2.1 for hydrogen-oxygen mixtures and Figure: 2.2 for hydrocarbon mixtures such as methane-oxygen [14].

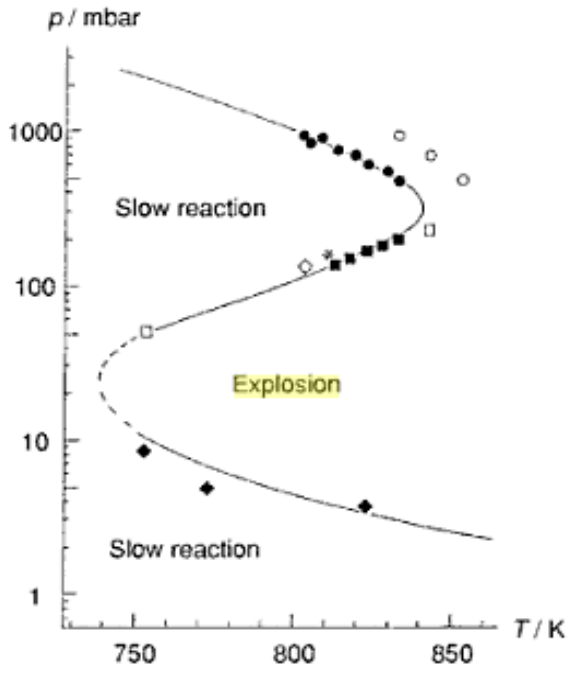

Figure 2.1: p-T Explosion Diagram for a Hydrogen-Oxygen Mixture (Maas and Warnatz, 1988)

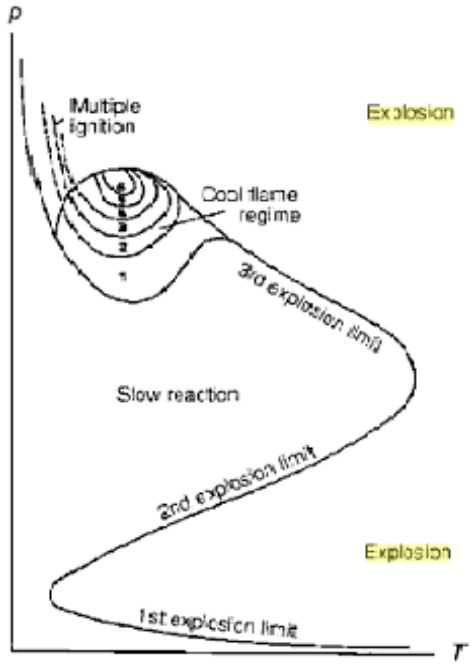

Figure 2.2: p-T Explosion Diagram for Hydrocarbon Mixtures (Warnatz, 1981)

Chapter 3: Experimental Procedure and Design

3.1 Materials and Design

The materials most involved with the design concepts are the impact apparatus and the specimen chosen for the experiment. The apparatus contains many parts and utilizes two nozzles designed for two major types of tests: A Cold Fire Test Nozzle (CFTN) and a Vitiated Heating Test Nozzle (VHTN). In each test, there are similarities and differences as the experiment is performed.

Multiple measurement devices are used to find data on the performance of the apparatus. An example of this includes the measurement of the velocity of the alumina particle exiting the tube from the CFTN and the VHTN. Temperature measurements of the specimen as well as the exit temperatures and chamber pressures of the VHTN and CFTN are taken for the purpose of comparing and investigating the exposure of the specimen.

3.1.1 Impact Apparatus

The impact apparatus consists of two major parts: 1) nozzle 2) mounting stand assembly. Two separate nozzles are constructed to perform a cold fire and hot fire test. The entire assembly was carefully designed and in a few cases redesigned. All parts and assemblies were designed using UGS.NX 4 CAD Software.

Mounting Stand and Assembly

The mounting assembly, shown in Figure 3.1 shows a simple method of how the nozzle mounts and adjusts within the mounting assembly. The specimen is no more than half an inch in diameter so the adjustments only need to be a minor in either direction. The mounting assembly consists of four rods and three plates, two of which keep the assembly stable and rigid. The middle plate allows the nozzle to adjust vertically while the two l-brackets adjust the nozzle horizontally.

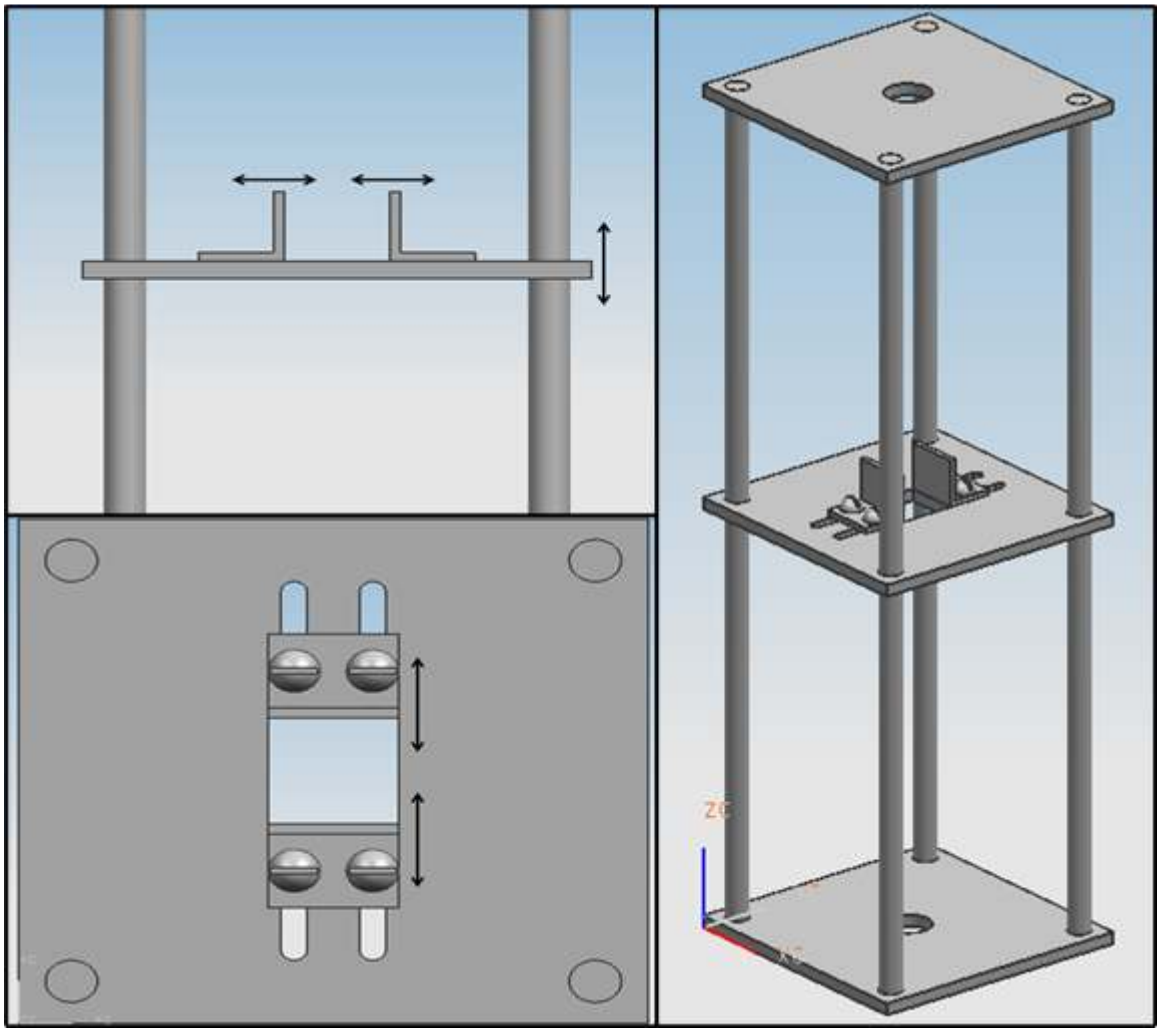

Figure 3.1: CAD Model of the Mounting Stand

The entire assembly is constructed out of 304L stainless steel. A stainless steel c-clamp is used to secure the nozzle in place once the l-brackets are secured along the sides of the nozzle. Once the nozzle is in place, the middle plate is kept level and in place by four spherical clamps placed on each rod as shown Figure 3.2. The middle mounting plate is leveled before all the spherical clamps are secured in place. The middle plate is designed for each of the tests nozzles to be securely mounted.

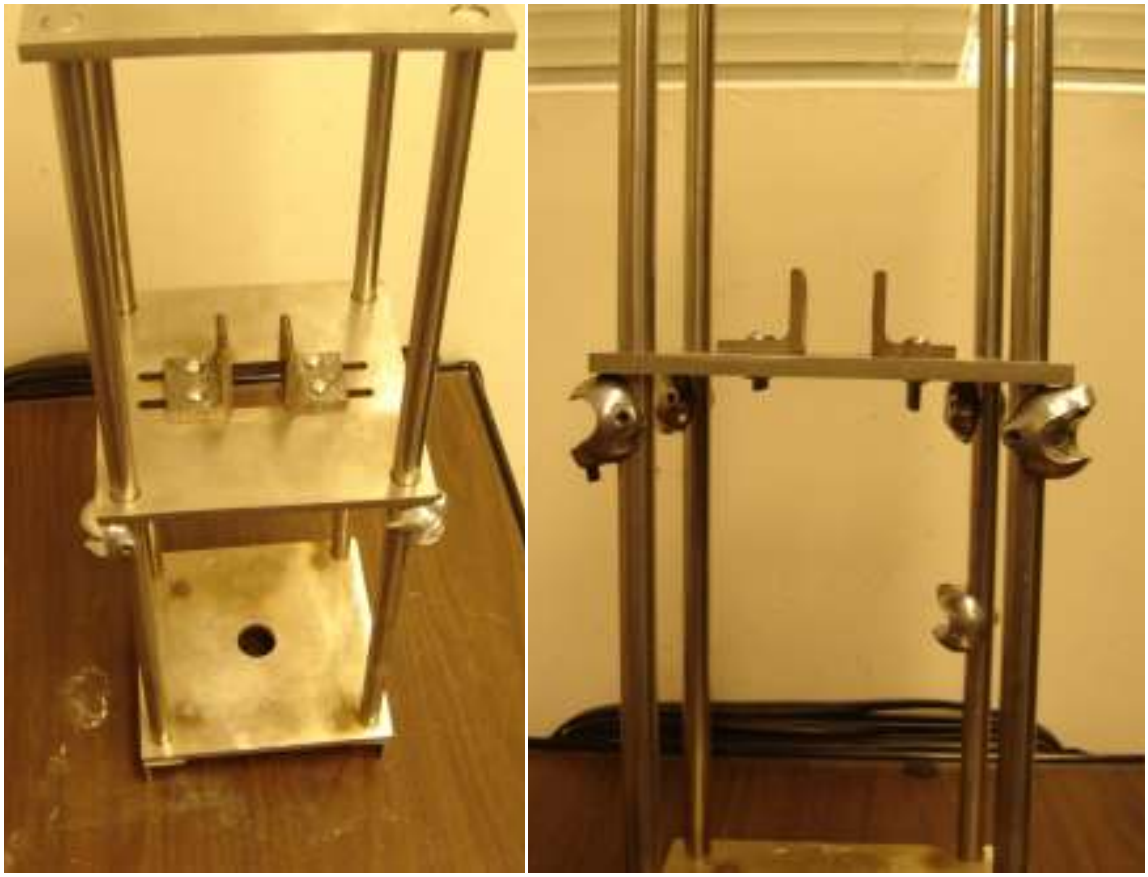

Figure 3.2: Test Stand Assembly

Cold Fire Test Nozzle

The CFTN is used to fire a particle without taking into consideration any thermal shock from the specimen at higher temperatures. Since nozzle is not directly exposed to heat, the material chosen for this nozzle is aluminum. The simple design of the nozzle shown in Figure 3.3 contains only two inlets and one outlet. One inlet, however, is only used to insert one particle each time the experiment is tested. During the experiment, this inlet is sealed off. During the cold fire tests, Nitrogen is used at various pressures to propel the particle through a ¼ in. OD and .18 in. stainless steel tube ID which acts as a barrel to increase the velocity and accuracy of the particle. The inlet and outlet, other than the particle inlet, are only used to pass nitrogen and propel the particle. As seen from the diagram, the particle sits off to the side of chamber, and as the nitrogen passes through the chamber, the particle is forced out of the nozzle and through the tube. Figure 3.3 also shows how the inlet for the particle is sealed off using a

small screw.

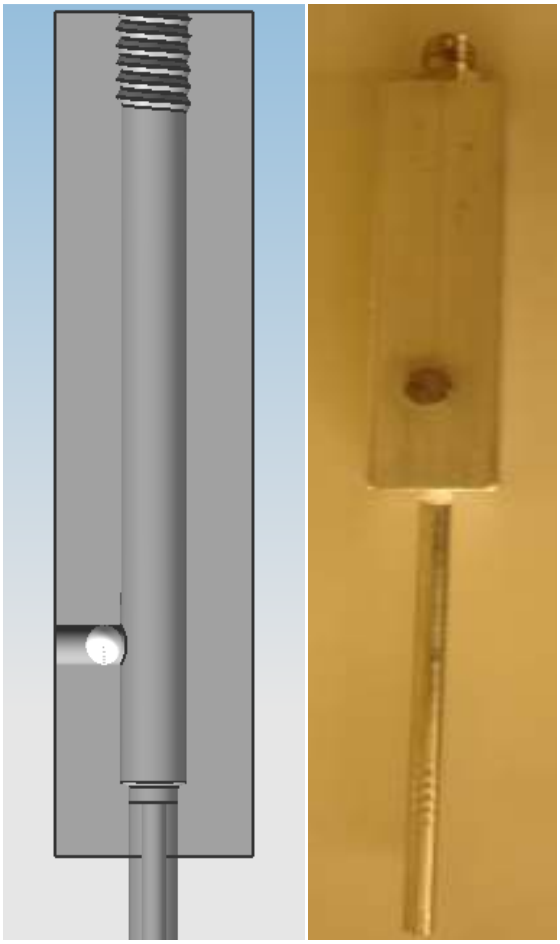

Figure 3.3: CAD Model and Actual Model of the CFTN

The inlet of the nozzle contains a 1/8-inch NPT tap while the outlet of the nozzle The barrel is threaded directly into the nozzle further decreasing the inside diameter and reducing the distance between the end of the tube and the specimen.

Vitiated Heating Test Nozzle

The VHTN is a much more complicated version of the CFTN. In the VHTN test, it is no longer assumed that thermal shock is not a factor; therefore, a vitiated heater is designed as combustion takes place within the chamber of the nozzle, heating the particle as the combustion between the two gases launch the particle. However, the exit temperature of the air in the VHTN is estimated to be around 400

°C still giving the opportunity for thermal shock to be a factor. As in the CFTN, measurements are taken to find the capabilities of the design. However, in the case of the VHTN, care must be taken to not over exceed the capabilities of the material or equipment used for measurements.

The diagram of the VHTN in Figure 3.4 shows that the particle is inserted differently than the CFTN. In this test, the particle sits inside the oxygen line. It was the intent for the particle to be propelled from the combined pressure of methane and oxygen as well as the initial combustion from the two gases. The nozzle contains a total of five inlets and one outlet. There three other ports built in to gather data when testing for the performance of the VHTN. Figure 3.4 shows the intent of every inlet, outlet, and ports.

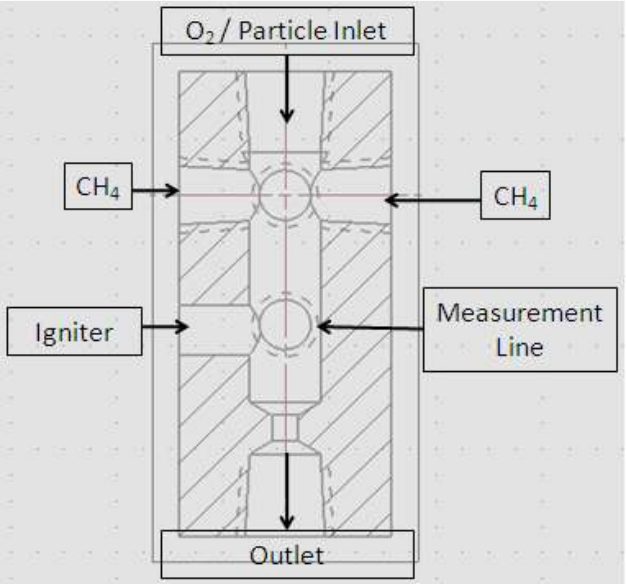

Figure 3.4: Schematic of the VHTN

The material used for the nozzle is 304L stainless steel. The material in this case must withstand the heat from the flame taking place in the nozzle chamber. Another important change in this design from the CFTN is the barrel. Since the tip of the flame is the hottest area of the flame, a stainless steel tube may not withstand the heat during the time needed to run the experiment. Taking into account the high temperatures, a mullite tube is used in substitute for stainless steel for its high melting point and

relatively high thermal expansion for a ceramic material. Another advantage of using the mullite tube is that it contains no electrical conductivity. When using the induction furnace, the tube may be as close as desired to the specimen without generating any heat from the induction furnace. As shown in Figure 3.5 the barrel is glued with a ceramic adhesive into a straight union. The thread of one end of the union is a 1/8 in. NPT. The NPT end threads into the outlet of the nozzle. The other end of the thread is a ¼ in. Swagelok tube fitting, however, the thread itself is not used.

Figure 3.5 Mullite Tube with

Figure 3.6 shows the entire assembly of the VHTN mounted within the mounting assembly. Little modifications were made to the mounting assembly for a secure fit of the nozzle. One minor modification includes a ¼ in. slit cut into the L-bracket to allow the igniter to slide securely. Figure 3.6 also illustrations the connections of the methane inlets. As the methane line splits into four different inlets, the line must be maneuvered in such a way that the stand does not obstruct the flow of methane into the chamber. One oxygen line connects directly into the nozzle chamber while carrying the particle within the line. As oxygen is released, the particle is also released.

Figure 3.6: VHTN Placed Securely into the Mounting Stand Assembly

Alumina Particle

The particle used for this experiment is an alumina particle. Each alumina particle used is between .017-.019 grams and between 2.05-2.20 mm in diameter. Table 3.1 and 3.2 show the momentum and kinetic energy of the particle at the mass specified velocity specified in the tables. The velocities used were measured as discussed later in this paper. The momentum equation was calculated as follows:

$$Momentum = mass \times Velocity$$

The kinetic energy was calculated as follows:

$$Kinetic\ Energy = \frac{1}{2}\ mass \times Velocity^2$$

Percent change in momentum was calculated as follows:

$$\%\ Momentum\ Change = \frac{Momentum\ Change}{Full\ Momentum} \times 100$$

It is noted that the percent change in momentum at each velocity is 10.53% between the two masses of the particle.

Table 3.1: Momentum of the particle at the Velocity and Mass Specified

Momentum (g*m/s)					
Mass (g)/ Velocity (m/s)	**44.3**	**50.7**	**64.4**	**72.5**	**80**
0.017	0.75	0.86	1.09	1.23	1.36
0.019	0.84	0.96	1.22	1.38	1.52

Table 3.2: Kinetic Energy of the Particle at the Velocity and Mass Specified

Kinetic Energy (mJ)					
Mass/Velocity	**44.3**	**50.7**	**64.4**	**72.5**	**80**
0.017	16.68	21.85	35.25	44.68	54.40
0.019	18.64	24.42	39.40	49.93	60.80

An alumina particle is used for its high melting temperature and to simulate an impact as a material hits random particles traveling at high speeds. During the cold test, the particle is only exposed to the heat from the specimen upon impact. In this case, the alumina is not subjected to extreme heat. In the case of the vitiated heating test, the high melting point of alumina becomes advantageous. The combustion that occurs within the chamber during the vitiated test runs exposes the particle to extreme heat at high velocities. Figure 3.7 presents an idea of the size of the particle as it is placed next to a penny.

Figure 3.7: Alumina Particle

3.1.2 $MoSi_2$ Specimen

The specimen used in this experiment is molybdenum disilicide ($MoSi_2$) shown in Figure 3.8. The $MoSi_2$ is applied due to the high melting temperature and brittle nature. The brittle nature of the $MoSi_2$ becomes beneficial as the damage is examined due to the impact of the alumina particle. The relatively high electrical conductivity allows the sample to heat up within the induction coils.

Figure 3.8: Polished Molybdenum Disilicide Specimen

The size of the MoSi2 sample is approximately .5 inches in diameter and .125 inches in thickness. The diameter of the specimen was required to be less than the diameter of the coils, however, a large enough surface area is convenient for repeatable impacts by the alumina particle. The thickness is chosen on the basis that visible damage from the impact occurs since the specimen is to be analyzed. Each specimen is sanded up 1200 grit sandpaper. Although scratches are apparent when examined under a microscope, it is not necessary to polish each specimen as the cracks are expected to be much larger than the scratches.

During each test, the specimen will not only endure an impact from an alumina particle, but is also exposed to high exit pressures from the propellants of the nozzle. The specimen is mounted securely to not disperse once the nitrogen or methane and oxygen gases are released. The specimen is

tested once the maximum temperature is reached, thus it is a hazard given that a hot specimen blown away due to an unsecured mount will cause serious injury if contact is made with human hands. An alumina crucible is constructed to mount the specimen securely and is designed with enough length to place the specimen within the coils of the induction furnace as shown in Figure: 3.9. The alumina crucible is made by cutting an alumina cylindrical block and drilling a ½ in. drill bit into the center. Since the alumina block is porous, the hole is drilled by hand with little difficulty.

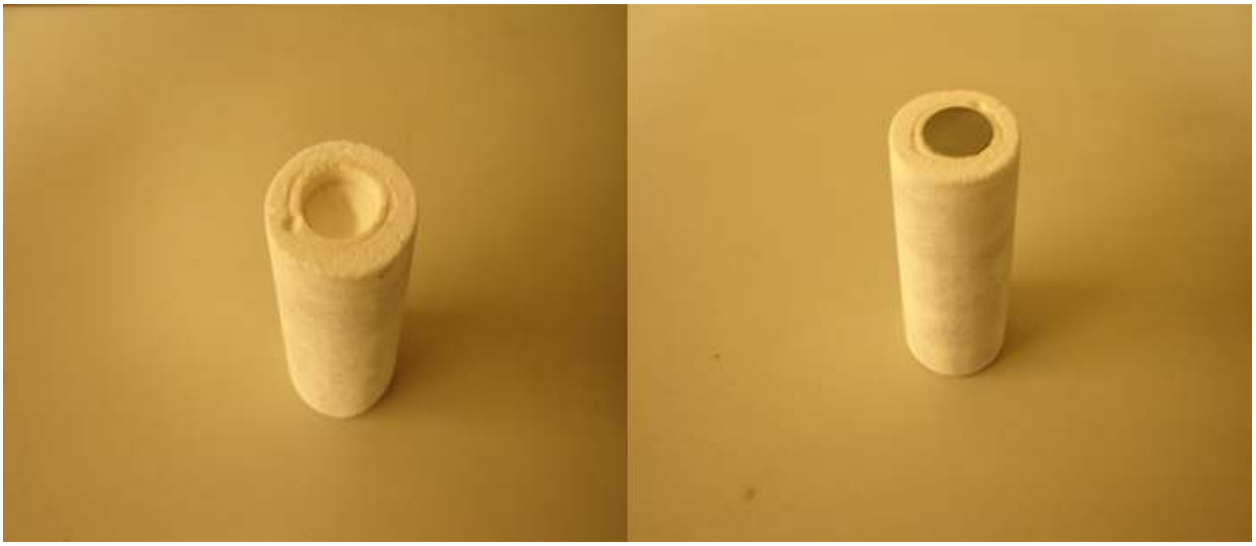

Figure 3.9: Alumina Crucible

3.2 Measurement Methods

The measurements taken on the impact apparatus are just as important as the final results of the impacted specimen. As more measurements are taken, more equipment is needed to produce the resultant measurements. In this case, the measurements include the following:

1. Velocity of the particle fired from the CFTN and VHTN.
2. Chamber pressures of the CFTN and VHTN.
3. Exit temperature of the VHTN and CFTN
4. Time required for the specimen to reach maximum temperature

3.2.1 Particle Velocity Measurements

The method of finding the velocity is different for the vitiated heating and cold tests. Measurement of the particle fired from the CFTN took an electrical approach as optical switch sensors were used to find the time travelled between two points. Due to the higher temperatures of the VHTN, a different approach of using a high speed camera is used to measure the velocity of the particle as it leaves the mullite tube. In both cases, calibration plots are generated from the velocity data.

Particle Velocity Measurements Fired from the CFTN

The particle in the CFTN is measured using two slotted optical switches as shown in Figure 3.10. The idea behind using the optical switches is to find the time difference when the particle passes through both of the switches separated by a known distance. Each switch contains an infrared Light Emitting Diode (LED). As the particle passes through the LED, the voltage of the sensor drops to zero. The voltage of each sensor is measures using an oscilloscope.

Figure 3.10: Slotted Optical Switch

Each switch contains a .375 inch slot giving plenty of room for the ¼ in. stainless steel tube to fit in between. Two holes are drilled 15.25 inches apart on both sides of the tube and the optical

switches are mounted such that they are securely placed in order for the laser to pass through the small hole as illustrated in Figure 3.11. The illustration in Figure 3.12 shows the particle passing through points 1 and 2. The switches are powered using two power supplies, supplying 5 volts each. A breadboard in Figure 3.13 shows the wiring to power each switch independently and display the power output onto an oscilloscope.

Figure 3.11: The Positions of Both Switches Placed on Tube

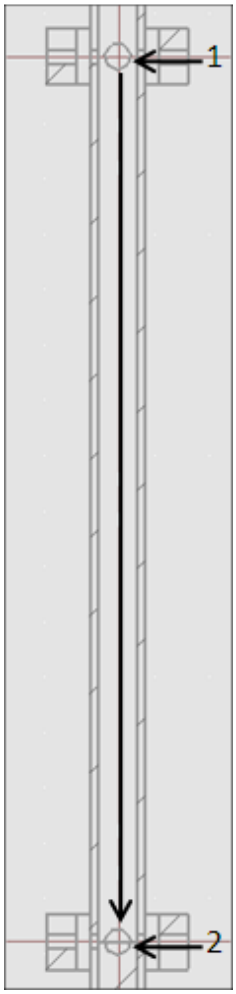

Figure 3.12: Illustration of the Particle as it Moves Past the Sensors

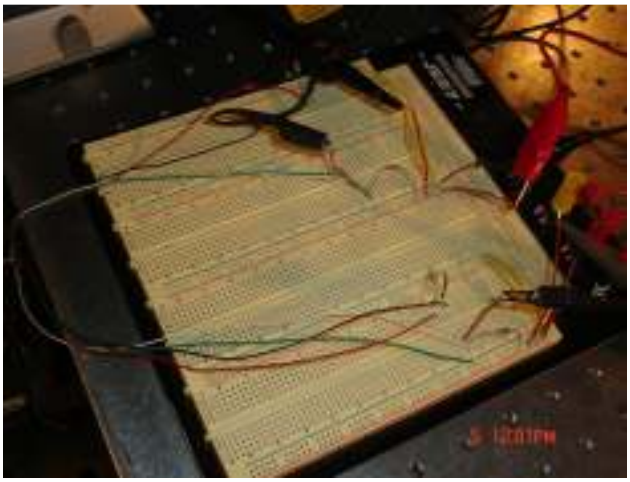

Figure 3.13: Breadboard Connecting the Velocity Measuring Equipment

To measure the velocity of the particle, the nozzle is setup specifically to mount the optical switches in the correct position. The setup showed in Figure 3.14 shows how each piece of equipment connects together to work as a measuring device. Other pieces of equipment include a vice grip to keep the nozzle in place along with the stainless steel tube. The nozzle must be securely placed as any small movements of the nozzle will change the position of the tube thus disrupting the optical switches.

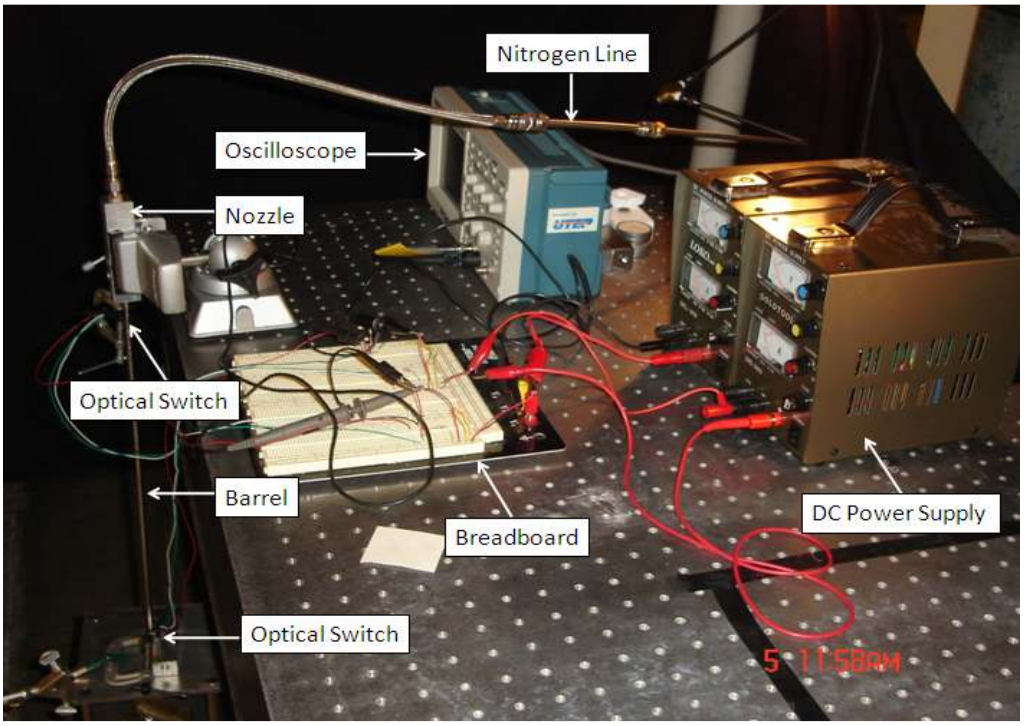

Figure 3.14: Particle Velocity Measurement Test Setup

The calibration plots are generated as shown in Figure 3.15. The plots are generated by measuring the particle velocities at five separate pressures, ten separate times at each pressure for a total of fifty velocity points. The average particle velocities at each pressure are calculated and are also plotted to show the variability at each pressure.

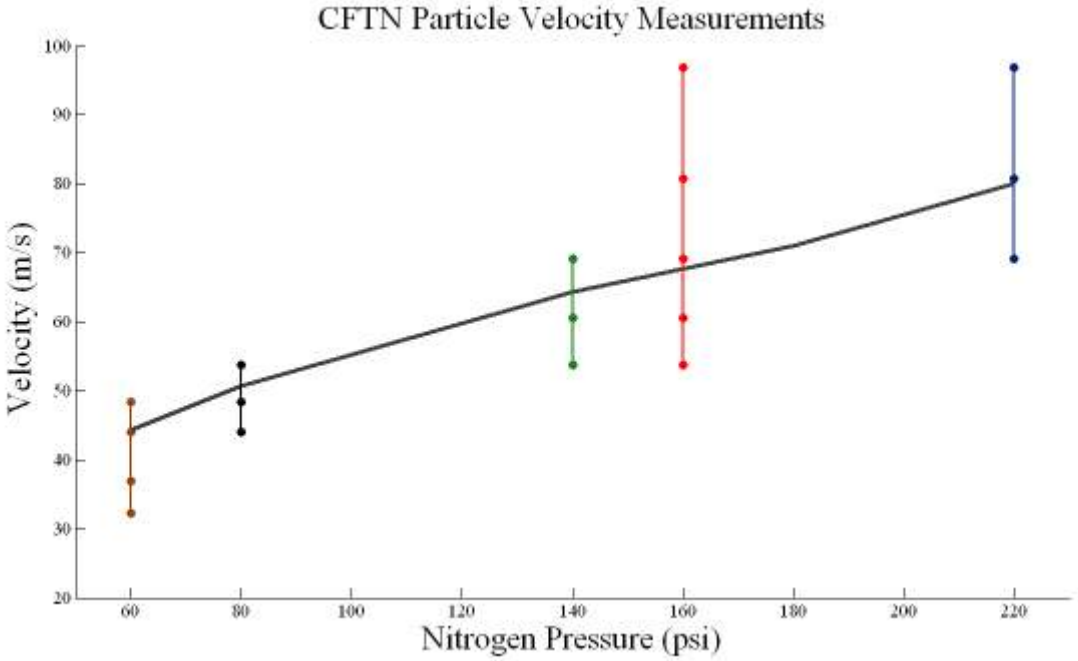

Figure 3.15: Data Collected at Each Pressure of Nitrogen

The velocity graph shows that the average velocities calculated maintain a somewhat linear form. There is a significant amount of variability in the case of the particle velocity at 160 psi and 60 psi. This may be due to the particle insertion method for the CFTN. The particle is placed off to the side as shown before in Figure 3.3. This may cause issues in that the particle may hit the walls within the chamber as the particle is introduced into the chamber. Since the bouncing of the particle within the chamber would be random, the exit velocity points may also result in scattered data. Due to the scatter, an error percentage was calculated to observe the maximum and minimum error points associated with the data during calibration. An average error is also included in the table. Table 3.3 shows the error assuming the calibrated velocity as the true velocity as indicated.

Table 3.3: Error Calculation by the Optical Switches

Optical Switch Error Calculations					
Calibrated Velocity (m/s)	**44.33**	**50.77**	**64.37**	**74.15**	**80.01**
Max % Error	27.18%	13.29%	16.42%	30.60%	21.04%
Avg % Error	9.22%	7.17%	5.97%	13.19%	5.42%
Min % Error	0.71%	4.62%	5.97%	6.71%	0.86%

Particle Velocity Measurements Fired from the VHTN

As stated earlier in this paper, high temperatures introduce problems not taken into consideration when dealing at room temperatures. This becomes the case when attempting to measure the velocity of the particle via the VHTN. The optical switches are designed with a 40° C ~ 80° C operating temperature. Since the fuel in this case is methane and oxygen as the oxidizer, temperatures of well above the operating temperature of the optical switches are predicted.

The Photron FASTCAM Super 10K (Figure 3.16) high speed camera is used to capture the particle as it fires out of the tube of the VHTN. The high speed camera can capture up to 10,000 frames per second (FPS). The process of capturing the particle traveling at a relatively high speed becomes tedious when triggering the high speed camera. The combination of the high velocity as well as the small size of the particle cause issues when capturing the particle traveling out of the tube. In addition, once the particle is captured, it may difficult to see the particle pass by while watching the recording of the high speed camera.

Figure 3.16: Photron FASTCAM Super 10K High Speed Camera

Although a high speed camera may catch video of the particle, a method of measuring the particle remains the challenge. It was concluded that a fiberglass screen would suffice to act as a grid. The grid is displayed in Figure 3.17 showing how the end of the mullite tube is aligned with the grid. The grid contains 1/8 in. x 1/16 in. rectangles; however, the 1/16 in. dimension is used to measure the passing particle. In this setup, it is important for the screen to directly face the tube. Another important

note is to place the screen immediately after the tube otherwise the high speed camera would view the screen at a different distance than the tube and particle. This would ultimately cause the velocity to seem slower as the grids would appear larger due to the perspective of the high speed camera.

Figure 3.17: Image taken from the High Speed Camera Depicting the Grid and Tube from the VHTN

The velocity results for the VHTN are presented measured utilizing a more visual tactic. An illustration in Figure 3.18 demonstrates the method the velocity is measured through the uses of the high speed camera. The time difference between each stage is .0001 seconds of 10,000 fps. As shown from the figure, there are two separate stages for a total of .0002 seconds between the two stages. As stated previously, the width of each grid is 1/16 of an inch. Looking very closely to the figure, it can be concluded that there are at total of 13 grid lines in which the particle passes through. A simple calculation shown can be used:

$$\frac{number\ of\ grids\ (in.)}{number\ of\ frames} * \frac{.0254\ m}{1\ in.} * \frac{1\ frame}{.0001\ s} = Velocity$$

In the case of Figure 3.17, the velocity is measured to be 103.188 m/s.

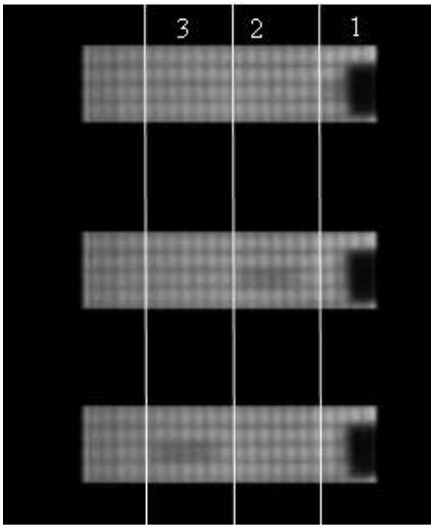

Figure 3.18: Process of Measuring the Velocity

The amount methane pressure is .57 times that of oxygen and was chosen for safety purposes and to reliably achieve a combustion and initial flame temperature. Similar to the CFTN, calibration plots are generated by firing ten particles at each pressure combination. In addition, averages are taken and are assumed to be the impact velocities during the final tests. The calibration plot is shown in Figure 3.19.

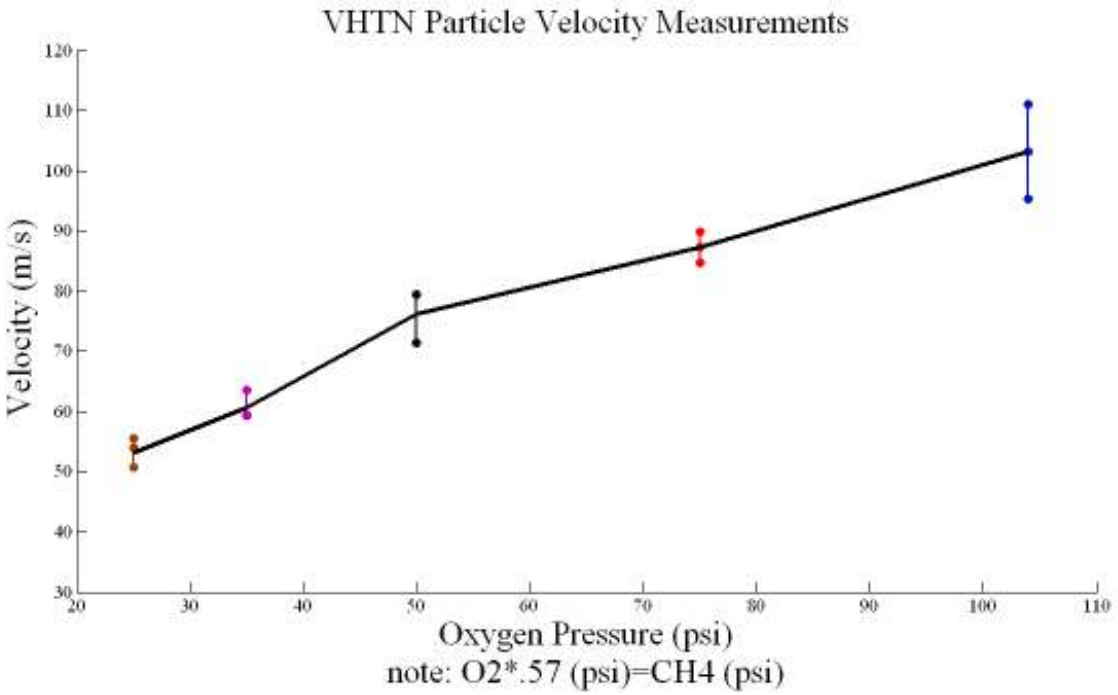

Figure 3.19: Figure Illustrating the Variability at Each Pressure

Similar to the CFTN, the increase in velocity is somewhat linear to the pressure increase. The difference lies in the rate at which the velocity curve increases. The repeatability of the velocity of the particles also seems to be consistent. Few outliers occur and the most variable velocity occurs at points of 75 psi oxygen (42 psi methane) and 25 psi oxygen (14 psi methane). The results may seem consistent due to the subjective nature of the measurement. Contrary to the CFTN, the particle is introduced directly into the oxygen line. This allows a direct inlet for the particle limiting contact from the particle to the walls of the nozzle chamber.

3.2.2 Exit Temperature of the VHTN

Reliably measuring the exit temperature of the vitiated heating test nozzle becomes important when investigating the thermal shock of the specimen. The use of a type S-thermocouple is used alongside the National Instruments USB-9263 10V Analog Output Module DAQ (Figure 3.20). The DAQ records temperature measurements at 12 Hz. The type S- thermocouple, as shown in Figure 3.21, is placed beneath the tube as exhaust flows passed the thermocouple thus measuring the exit temperature. Although achieving higher exit temperatures are desired, it is also important to keep in mind the hazards involved as higher temperatures are reached.

Figure 3.20: NI USB-9263 10V Analog Output Module

Figure 3.21: S Type Thermocouple Placed Directly Beneath the Mullite Tube

3.2.3 Heating of the Specimen

Multiple methods were investigated as to how the specimen would be heated while working efficiently with the impact apparatus and all the components involved. The use of the a 3 kW RDO Induction Heating Furnace equipped with a five turn heating coil (Figure 3.22) proved to be the most effective method of heating the specimen as well as giving the entire apparatus the freedom of adjusting to the placement of the specimen. As in most induction heating processes, the coils are water cooled during the heating process.

Figure 3.22: RDO Induction Heating Furnace and a Five Turn Heating Coil

The Induction Heater offers the advantage of heating the specimen without coming into contact with the specimen itself. Figure 3.23 shows the placement of the crucible within the coils as the CFTN is properly aimed at the specimen. Another advantage is the electrical conductivity of the specimen. Induction heating operates mainly with electrical conductive materials and in most cases induction heating is meant to melt materials. The high electrical conductivity of the $MoSi_2$ specimen allows for a wide variety of temperatures and including the option to surpass the melting point.

Figure 3.23: Test Setup with the Assembly and Furnace

3.2.4 Temperature Measurement of the $MoSi_2$ Sample

The method of measuring the temperature proved to be one of the greater challenges in that most methods of measuring temperature are through the means of a thermocouple. Since most thermocouples are electrically conductive, any thermocouple placed within the coils will heat the thermocouple according to the type of metal used. This causes inaccurate readings and may cause damage to the thermocouple.

Several methods were utilized to measure the temperature each with its own advantages and disadvantages. One method is measuring the temperature of the specimen through the use of an Electrophysics PV320T Thermal Camera (Figure 3.24). The IR camera proved useful in finding multiple temperature points of the specimen, creating graphs to show and find the time where the heat of the specimen reaches steady state, and take images and video during the heating process. As there are many benefits in using the IR camera, the primary set back was the lack of temperature range built into the system. The manufacturer states an accuracy range from -25 °C to 500 °C which is well below the maximum temperature required for the experiment.

Figure 3.24: Electrophysics PV320T Thermal Camera

The next method of temperature measurement for this experiment was the use of the use of a type-s thermocouple. The Thermocouple is placed directly on the surface of the specimen as shown in Figure 3.25. This becomes difficult in that the thermocouple must be placed in such a way that the

platinum and rhodium is not exposed to the magnetic field within the coils. This may cause a false reading and may damage the thermocouple. This thermocouple is utilized to reach higher temperatures than the thermal camera. The thermocouple is still limited in finding higher temperature limits as most working type-s thermocouple contain a range of around 1400 °C. In order to avoid damage to the thermocouple, temperatures around 1000 °C will be examined.

Figure 3.25: Type-S Thermocouple Placed on the Specimen

3.3 Impacting Testing

3.3.1 Test Setup

Each piece of equipment is gathered and placed in its proper order before performing the experiment. After each test is run, certain components including the impact apparatus are placed aside to access the specimen after it has been impacted. In order for accuracy, the induction furnace is set and the nozzle is aimed at the specimen. The simple schematics in Figure 3.26a and 3.26b show the relative positions of each component as the tests are run. In 3.26a, a push button valve is used for quick release time and firing of the particle. ¼ turn Swagelok valves are used for both tanks in the VHTN setup. Quick release of the oxygen or methane is not necessary in the case for the VHTN tests.

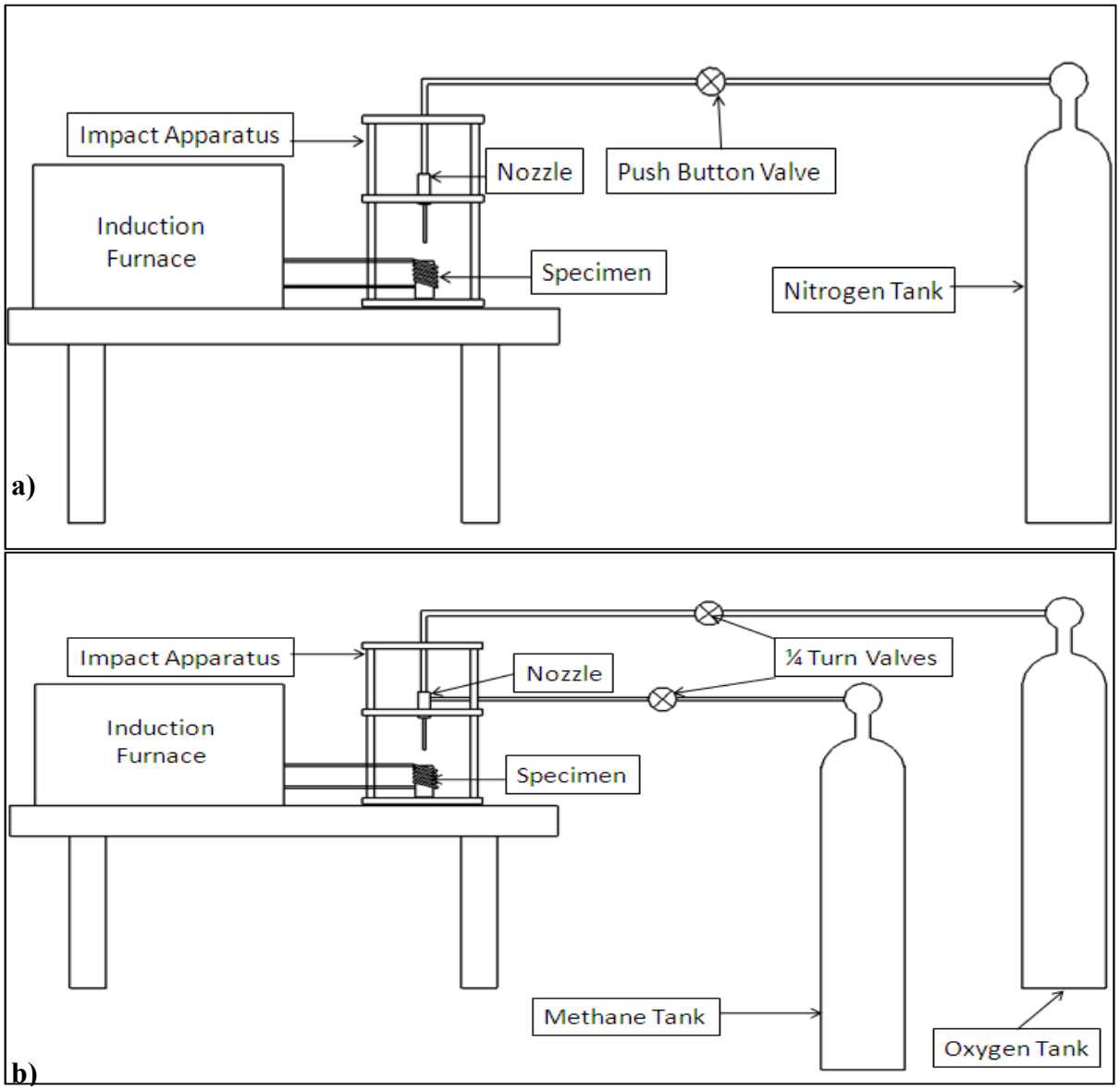

Figure 3.26: Schematic of the a) CTFN Setup b) VHTN Setup

Figure 3.27 shows the actual test setup used in the experiment. The VHTN is setup in this figure and shows how each tank is placed to interchange the connections when switching from the CFTN setup and the VHTN setup. It is also noted that a small Plexiglas shield covers the tube of the nozzle to block and particles or other hazards that may occur.

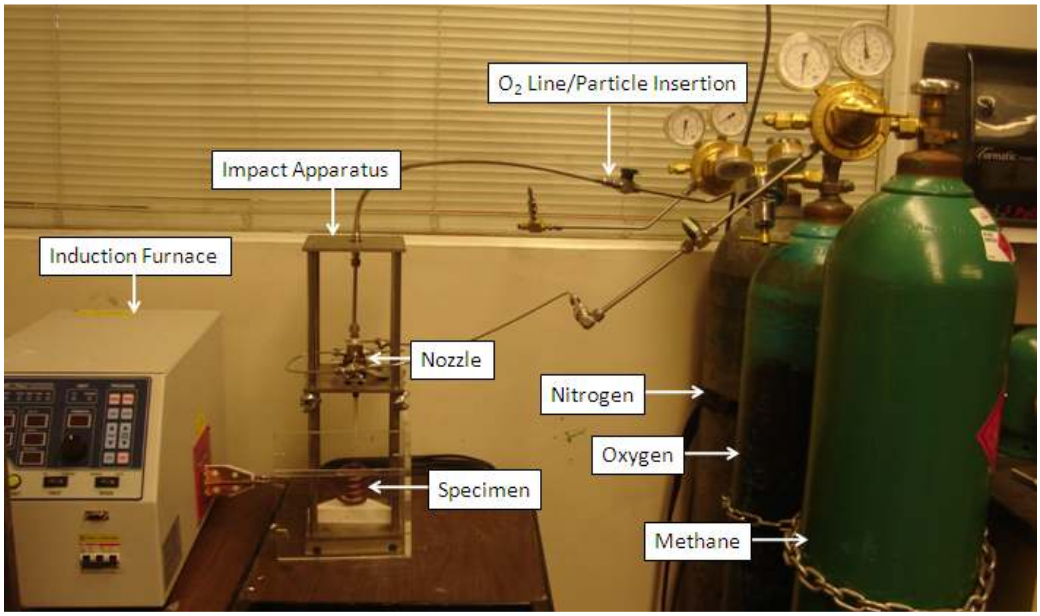

Figure 3.27: Test Setup

3.3.2 Test Process

Specimen Temperature Process

The temperature of the specimen is measured before any impact test run. The thermal camera is placed on the middle plate facing toward the specimen. The thermal camera measures the temperature of the specimen every second and the time to reach the maximum is determined from the plot. The repeatability of the maximum temperature is observed meanwhile the time to maximum temperature is taken into account. The time to maximum temperature determines the amount of time the specimen is heated before the particle is released from the nozzle.

CFTN Impact Test Procedure

The impact test using the CFTN is a straight forward process as nitrogen is the only propellant in the test. The test matrix in Table 3.3 shows the variety of pressures used to find the characteristics of the impact upon the MoSi2 specimen. The velocities of the particle are first tested to check the variability and repeatability at each pressure. Ten runs at each pressure are tested to find the average

particle velocity. During the impact tests, the velocity measurement is not recorded due to the obstructions associated with the optical switches and the rest of the measuring components. It is assumed that the calibration velocities measured from the ten runs are the velocities impacting the specimen during the impact tests. Three runs per pressure are tested to observe the damage of the specimen relative to the temperature and velocities.

The specimen is properly aimed using a laser pointer before the nitrogen line is connected. The laser is projected onto the specimen and the proper adjustments are prepared by shifting the impact apparatus and/or nozzle to where the laser points near the center of the specimen. The specimen is heated for the time duration to reach maximum temperature. Once maximum temperature is achieved, the set pressure is released through the use of a push button valve instantly releasing the particle. A stainless steel push-button valve (normally closed) aids in limiting the specimen from the exposure of cold nitrogen. Contrary to a "turn valve", the push button valve quickly closes as soon as the button is released offering a more convenient way of closing the nitrogen tank

Table 3.4: Test Matrix for the CFTN Impact Test

CFTN Impact Test		
Trial	**Pressure**	**Propellant**
1	60	Nitrogen
2	60	Nitrogen
3	60	Nitrogen
4	80	Nitrogen
5	80	Nitrogen
6	80	Nitrogen
7	140	Nitrogen
8	140	Nitrogen
9	140	Nitrogen
10	160	Nitrogen
11	160	Nitrogen
12	160	Nitrogen
13	220	Nitrogen
14	220	Nitrogen
15	220	Nitrogen

VHTN Impact Test Procedure

The process of testing the VHTN proves to be a much more involved process when compared to testing the CFTN. The process of constructing the test matrix (Table 3.5) is similar however. The velocity, much like in the CFTN test, is measured before the actual impact tests. Ten runs at each pressure ratio are used to measure the velocity using the high speed camera. Video of each run is captured at 10,000 fps. The procedure of measuring the velocity is subjective due to the high speed of the particle. The measurement is purely visual as the particle passes through the 1/16 in. grids. Since he objective of the VHTN is only to prove that thermal shock may or may not exist, fewer test runs are attempted.

The process of firing the VHTN begins with aiming the tube with the specimen similar to the CFTN. A laser pointer is used to align the tube near the center of the specimen. The next step is to power the igniter. A spark igniter is constructed using platinum wire and an alumina casing. A 10kV, 27mA Evertron Neon Power Supply produces the spark shown in Figure: 3.28. A Resbond Ceramic Adhesive is applied on the opposite end of the spark to seal and prevent a short circuit from occurring. Methane is then released using a quarter-turn Swagelok valve at the desired pressure. Then the Oxygen is released quickly after releasing methane to avoid any excess gas to gather outside of the nozzle. Releasing the oxygen also releases the particle within the line. As the particle passes through the chamber, the oxygen ignites with the methane giving the particle extra thrust to achieve higher velocities.

Figure 3.28: Spark Igniter

Table 3.5: Test Matrix of the VHTN Impact Test piece

VHTN Impact Test		
Trial	**Oxygen Pressure psi**	**Methane Pressure psi**
1	25	14.25
4	35	19.95
6	50	28.5
8	75	42.75
10	104	59.28

Analyzing the Test Specimen

The test matrices shown in the previous sections involve the amount and type of damage the specimen sustains. A microscopic image of each specimen is taken before and after impact to see the amount of damage done. Under a microscope, the size of the indention is examined and measured as well as any other resultant cracks. In the event of the specimen fracturing, the size of the indention is still noted as well as the number of pieces resulting from the fracture.

Chapter 4: Results and Discussion

4.1 Exit Temperature of the CFTN and VHTN

4.1.1 CFTN Exit Temperature

The exit temperature for the CFTN is shown in Figure 4.1. The tank pressure at which the temperature measurement is taken is measured to be 60 psi of Nitrogen.

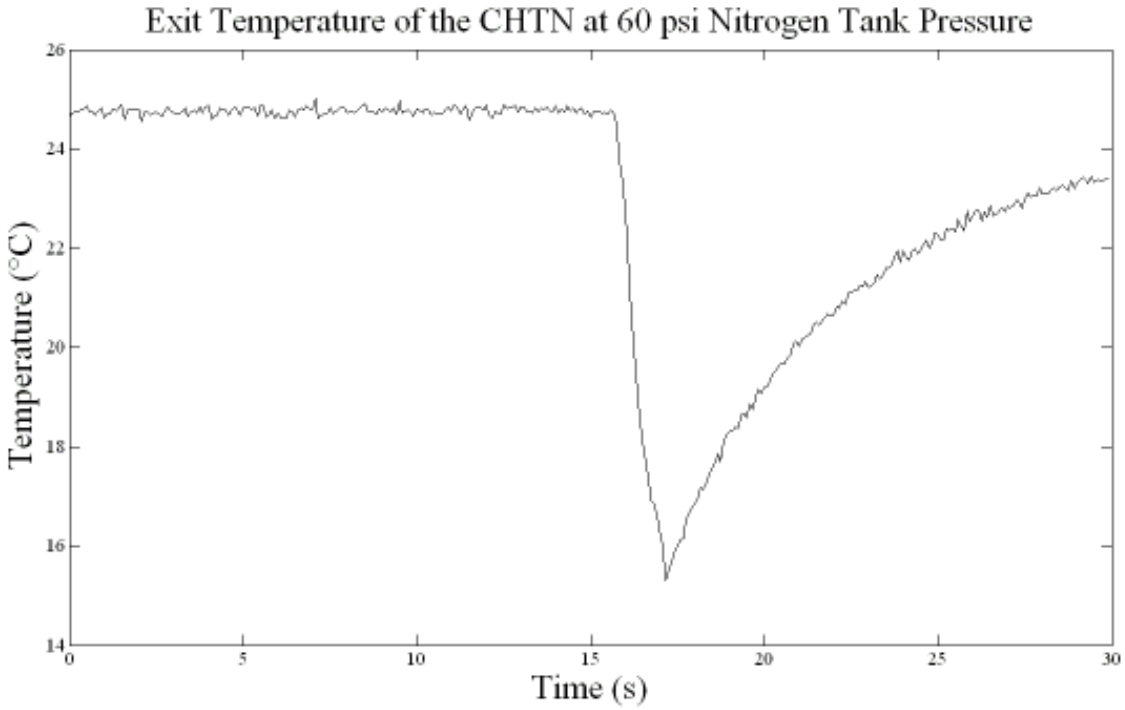

Figure 4.1: Exit Temperature Measurement with a Nitrogen Tank Pressure of 60 psi

Figure 4.1 shows about an 8 °C drop as the nitrogen is released. Exit temperature figures were taken at each of the pressures tested in the impact tests and are shown in Appendix A.

4.1.2 VHTN Exit Temperature

The exit temperature of the VHTN is taken in order to investigate the specimen's temperature exposure. Figure 4.2 shows the exit temperature from the VHTN with oxygen and methane pressures of 25 psi and 14 psi respectively.

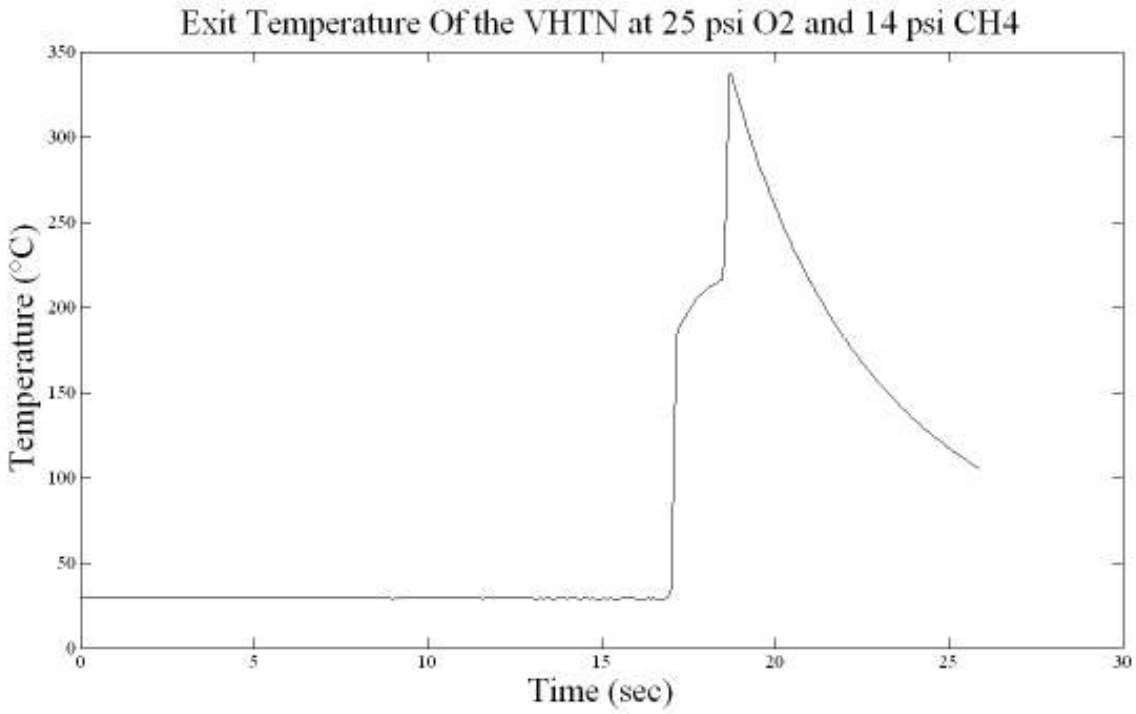

Figure 4.2: Exit Temperature of the VHTN with O_2=25 psi and CH_4=14 psi

Figure 4.2 shows the point at which the ignition occurs. Shortly after the ignition, the flame begins to cool. As the valves are closed, the lines left over gases in the lines are forced out creating a thrust with a higher temperature. In the case that there is a delay in closing the valves, the temperature may drop significantly from the initial temperature as the gases ignite. Plots are created at each test pressure and can be seen in Appendix B. The maximum temperatures achieved were limited to the strength of the mullite tube. Although mullite can withstand high temperatures, a few cases proved that that the mullite tube was unable to withstand the initial ignition from the methane and oxygen. As a result, pressure mixtures were varied to meet the capabilities of the mullite material.

4.1.3 Comparison

The comparison of Figure 4.2 and Figure 4.1 show a significant difference in temperature. Although the temperature drops in the VHTN, the exit temperature always remains higher than the exit temperature of the CFTN.

4.2 Temperature of the Specimen

The specimen is impacted at two different temperatures. The lower temperature measurement is taken using the infrared thermal camera and the higher temperature is measured using a type-s thermocouple along with a NI-9228 DAQ Assist. Figure 4.3 Shows the temperature curve of the specimen when the induction furnace is set to 3% power. Figure 4.4 shows an image taken from the thermal camera at 400 °C. Figure 4.5 shows a similar graph utilizing the thermocouple placed on the surface of the specimen. The point at which the specimen reaches steady state is the time where the particle is fired.

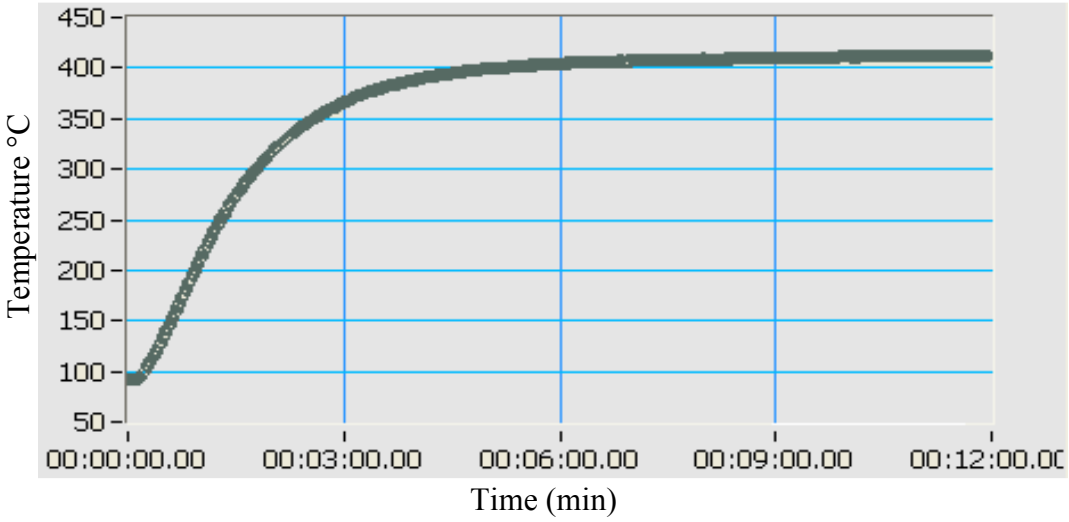

Figure 4.3: Temperature of the Specimen Measures by the IR Camera

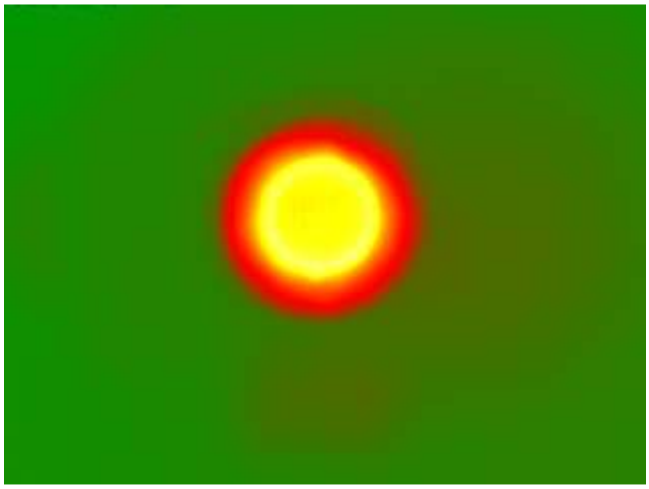

Figure 4.4: Photo of the $MoSi_2$ Taken by the IR Camera at 400 °C

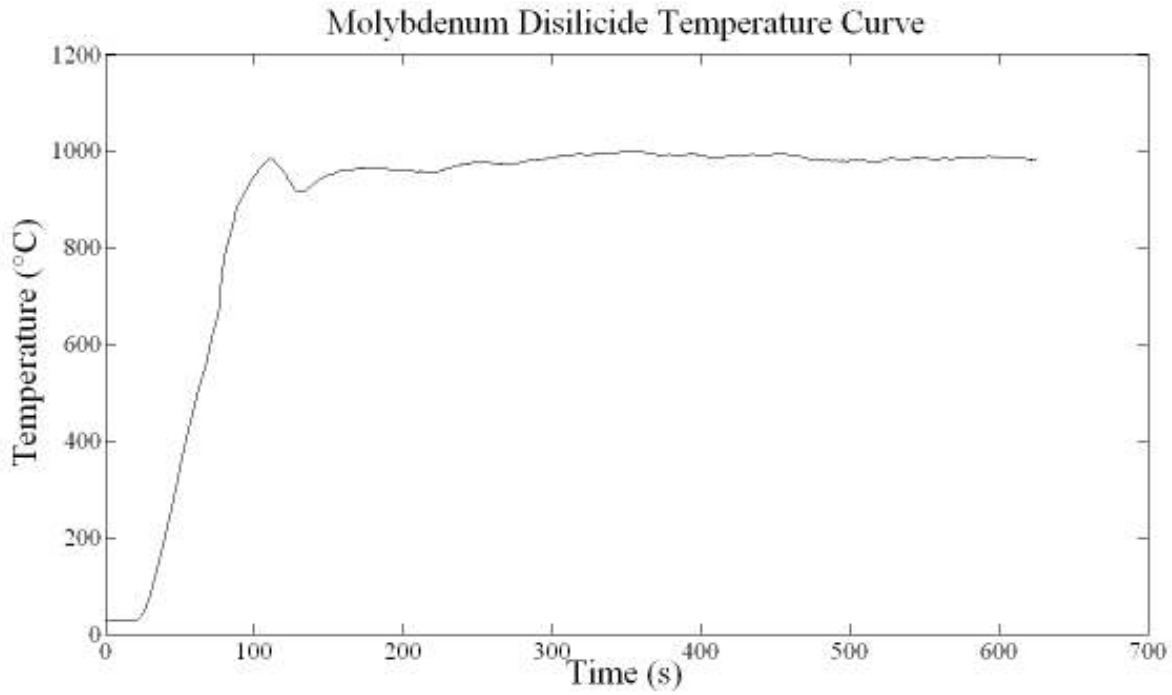

Figure 4.5: Temperature vs Time Curve of $MoSi_2$ Measured by a Type-S Thermocouple

4.2.1 Comparison

When using the IR camera, the average temperature of the area in Figure 4.3 is recorded to 413.3 °C. The maximum temperature within the area is recorded to be 472.8 °C while the minimum temperature was recorded at 390.6. Observing the graph shows the steady state temperature begins

around ten minutes. For this reason, the particle is fired at this point. In the case of the higher temperature, the maximum temperature recorded was 1001.8 °C. The fluctuation of temperature is shown in both graphs and is much more evident in the case of the higher temperature. This is caused by the fluctuation of the voltage as the power output is increased. Higher power outputs resulted in higher fluctuations in voltage during random moments. The electrical outputs applied for both the low and high temperatures are listed in Table 4.1.

Table 4.1: Electrical Outputs

Voltage	Current	% Power	Max Temperature
41	22	4	413.3
233	56	65	1001.8

4.3 Damage of the Specimen

The damage of the specimen is defined as the length of the indentation due to the impact from the alumina particle. Figure 4.6 shows a comparison of an impacted specimen at 400 °C and 220 psi with a specimen at 1000 °C at the same pressure. The lower temperature impact shows a more brittle nature as the specimen is broken into four pieces. The higher temperature specimen shows multiple secondary cracks, however, no fracture occurs. Figure 4.7 shows the process utilized to measure the damage length. The red line indicates the diameter of the indention and is measured onto a formatted picture with a ruler with units of microns. The red line shows a length of 620 microns or .62 mm. The impact lengths for the remaining specimens can be examined in Appendix C.

Figure 4.6: Impact at 400 °C (left) and 1000 °C (right)

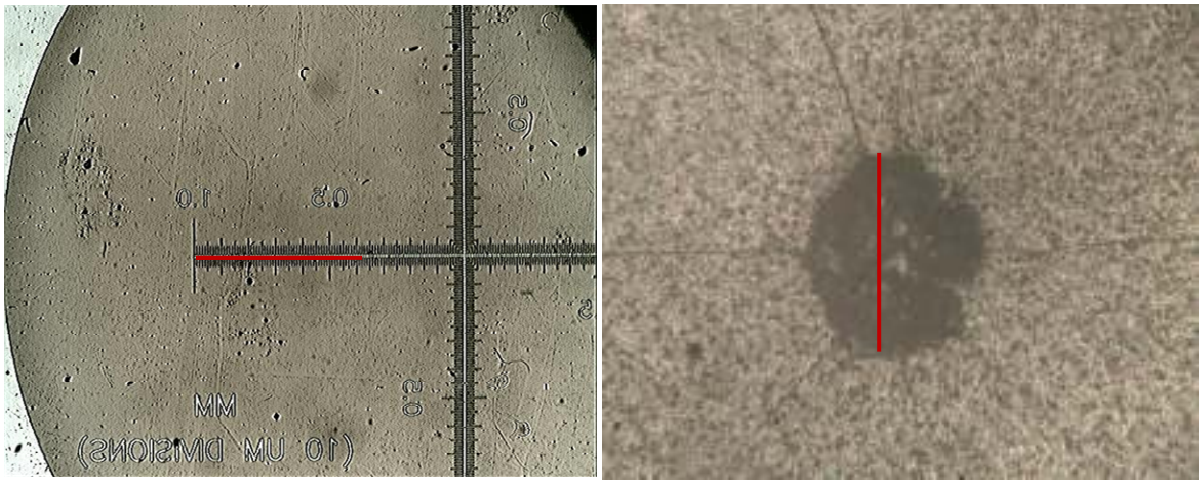

Figure 4.7: Length Measurement Method

Table 4.2 and Table 4.3 show the completed test matrices for temperatures 400 °C and 1000 °C using the CFTN.

Table 4.2: Completed Test Matrix for CFTN Experiment

CFTN Impact Test						
Trial	**Temperature °C**	**Pressure psi**	**Velocity m/s**	**Propellant**	**Impact Length mm**	**Number of Fractures**
1	400	60	44.33145292	Nitrogen	0.67	3
2	400	60	44.33145292	Nitrogen	0.7	None
3	400	60	44.33145292	Nitrogen	0.63	None
4	400	80	50.76632576	Nitrogen	0.7	None
5	400	80	50.76632576	Nitrogen	0.63	3
6	400	80	50.76632576	Nitrogen	0.65	None
7	400	140	64.36619544	Nitrogen	0.68	3
8	400	140	64.36619544	Nitrogen	0.7	4
9	400	140	64.36619544	Nitrogen	0.56	None
10	400	160	70.97573909	Nitrogen	0.75	3
11	400	160	70.97573909	Nitrogen	0.73	None
12	400	160	70.97573909	Nitrogen	0.61	None
13	400	220	80.00622024	Nitrogen	0.71	4
14	400	220	80.00622024	Nitrogen	0.7	None
15	400	220	80.00622024	Nitrogen	0.71	4

Table 4.3: Completed Test Matrix for the CFTN Impact Test at 1000 °C

CFTN Impact Test						
Trial	**Temperature °C**	**Pressure psi**	**Velocity m/s**	**Propellant**	**Impact Length mm**	**Number of Fractures**
1	1000	60	44.33145292	Nitrogen	0.665	None
2	1000	60	44.33145292	Nitrogen	0.58	None
3	1000	60	44.33145292	Nitrogen	0.54	None
4	1000	80	50.76632576	Nitrogen	0.62	None
5	1000	80	50.76632576	Nitrogen	0.62	None
6	1000	80	50.76632576	Nitrogen	0.665	None
7	1000	140	64.36619544	Nitrogen	0.62	None
8	1000	140	64.36619544	Nitrogen	0.71	None
9	1000	140	64.36619544	Nitrogen	0.71	None
10	1000	160	70.97573909	Nitrogen	0.62	None
11	1000	160	70.97573909	Nitrogen	0.71	None
12	1000	160	70.97573909	Nitrogen	0.71	None
13	1000	220	80.00622024	Nitrogen	0.75	None
14	1000	220	80.00622024	Nitrogen	0.62	None
15	1000	220	80.00622024	Nitrogen	0.75	None

Figure 4.8 shows the average damage length with respect to the particle velocity fired from the CFTN with a temperature 400 °C. Figure 4.9 also shows the average damage length with respect to the particle velocity fired from the CFTN with a temperature of 1000 °C. The variability in the crack lengths can also be examined and compared to the average. Figure 4.10 shows the temperature vs. velocity vs. damage length. This plot may predict the possibilities which may occur between the 415 °C and 1000 °C.

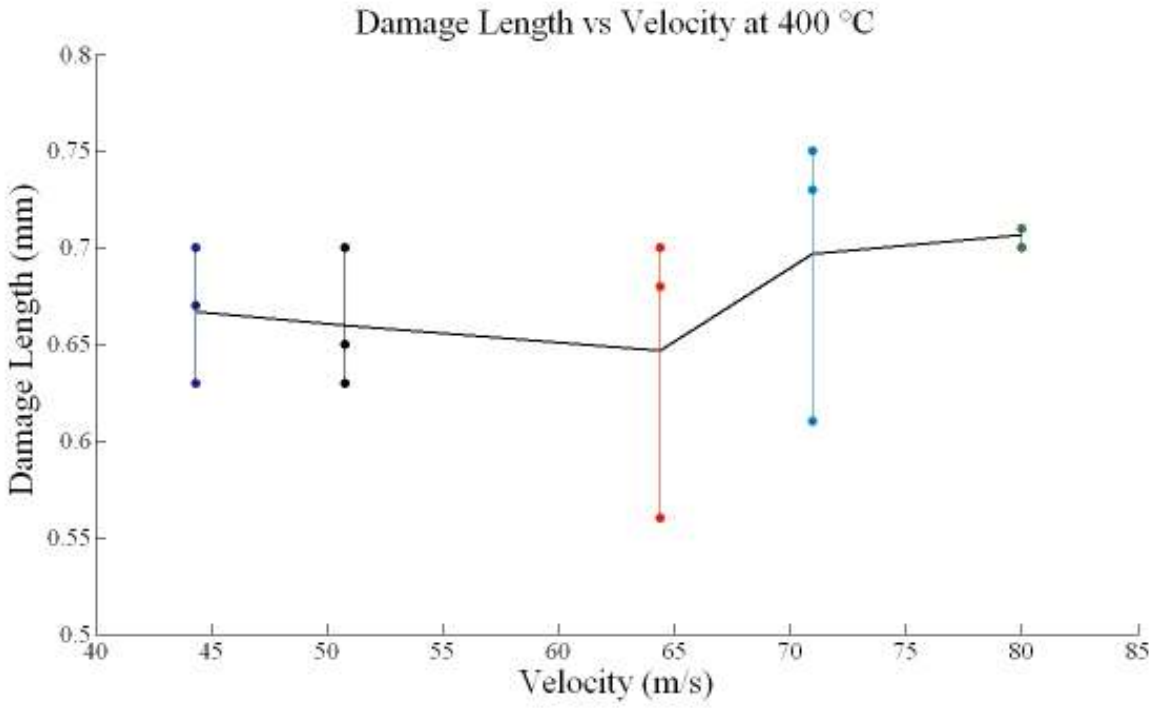

Figure 4.8: Damage Length Points with Respect to Velocity at 400 °C

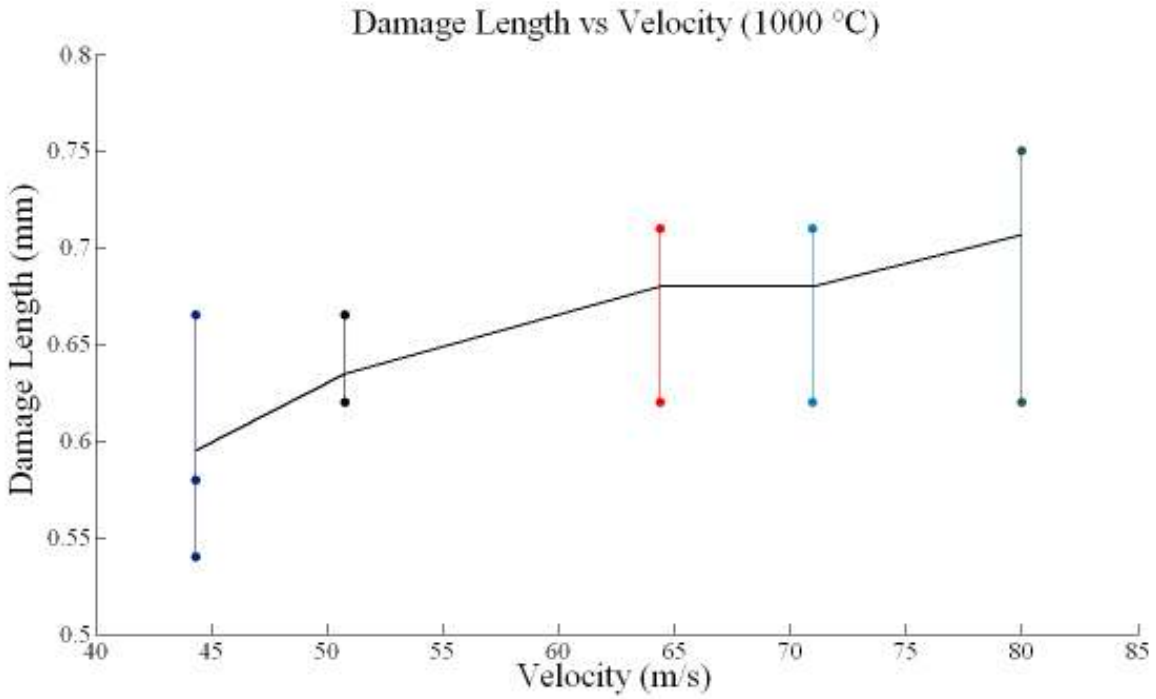

Figure 4.9: Damage Length Points with Respect to Velocity at 1000 °C

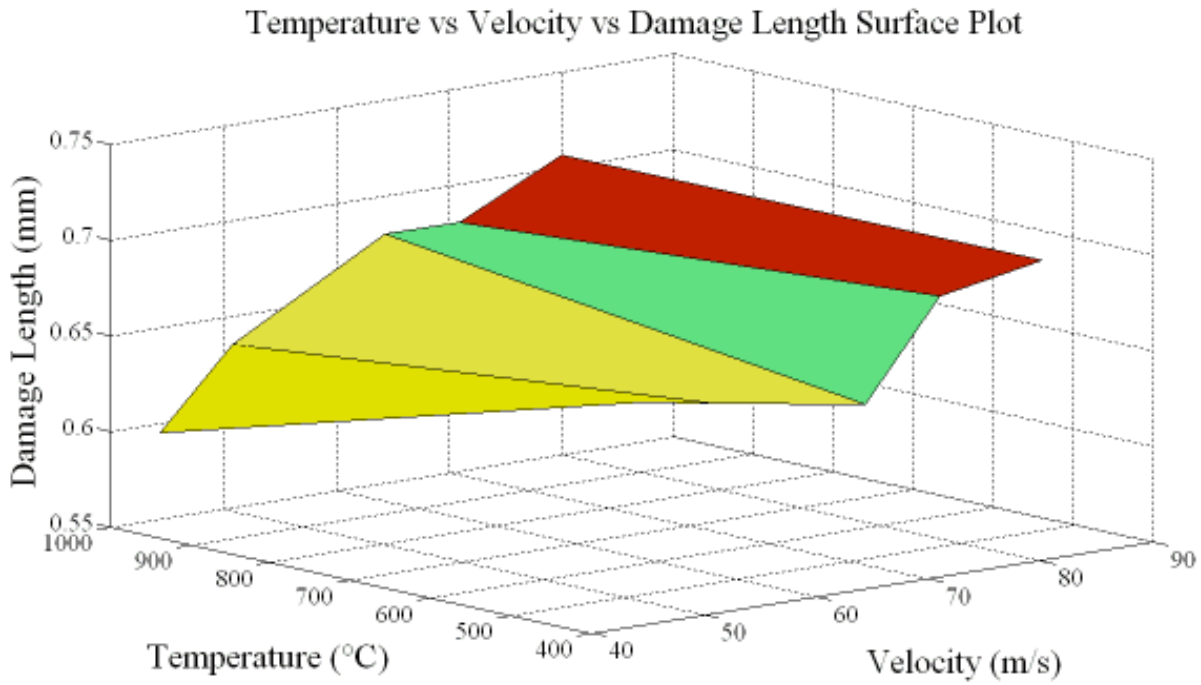

Figure 4.10: Surface Plot of Temperature vs. Velocity vs. Damage Length

Examining the combination of all the tables and plots from the impact tests, the damage done to the material at 400 °C does not necessarily increase as the velocity of the particle increases. This may be due to the brittle nature of $MoSi_2$ at lower temperatures. Although the impact does not increase at some points, the difference in damage length is relatively small. Between the first and second points, the difference is .001 mm and .02 mm between points 2 and 3. In the case of the specimen heated to 1000 °C, the damage length of the specimen increases with increase of the particle velocity. It is evident that the specimen becomes less brittle as secondary cracks and no fractures occur in the specimen.

4.4 Investigation of Thermal Shock

The thermal shock is examined by the VHTN and primarily at the temperature of 1000 °C. Table 4.4 shows the completed test matrix using the VHTN at 1000 °C. Figure 4.11 shows the plot of the velocity increase vs. the damage length.

Table 4.4: Completed Test Matrix of the VHTN Impact Test

VHTN Impact Test						
Trial	**Temperature °C**	**Oxygen Tank Pressure psi**	**Methane Tank Pressure psi**	**Velocity m/s**	**Damage Length**	**Number of Fractures**
1	1000	25	14	53.181	540	None
4	1000	35	20	60.667	650	None
6	1000	50	28.5	76.2	690	3
8	1000	75	42.75	87.297	700	3
10	1000	104	59.3	103.15	720	None

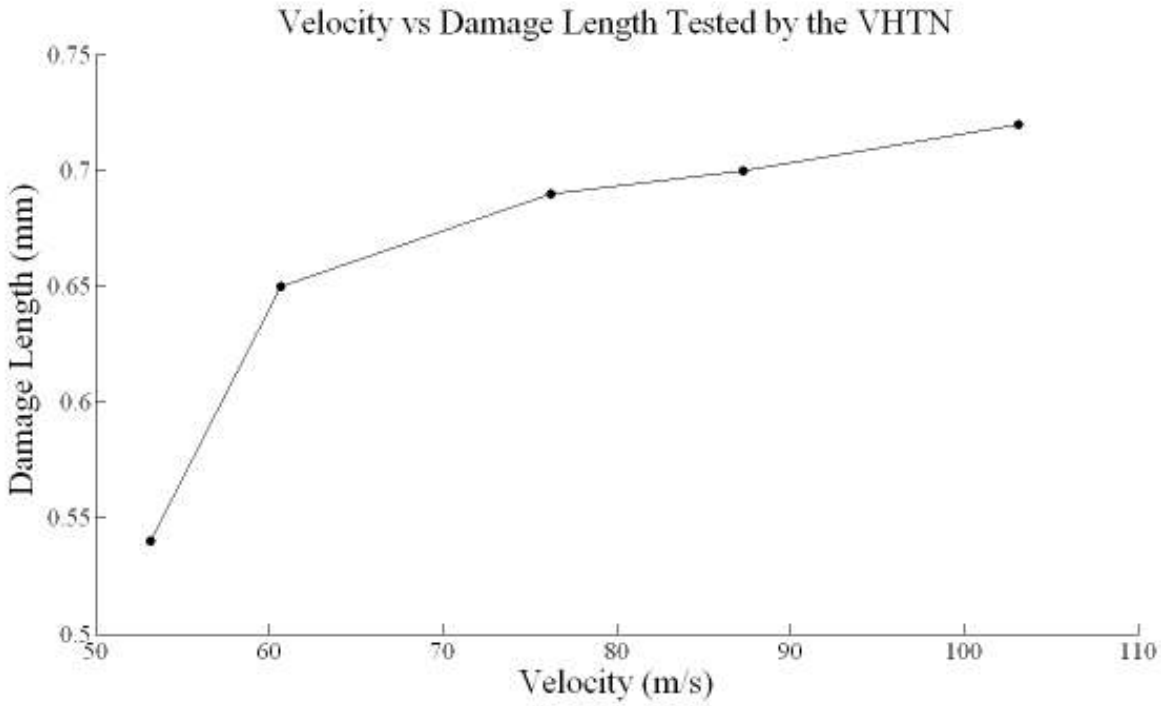

Figure 4.11: Impact Damage by the VHTN at 1000 °C

The comparison of Figure 4.11 to Figure 4.9 shows a close correlation of damage lengths. Although the resultant velocities of the VHTN are higher, the graph and table show a slightly larger damage length. This indicates the absence of thermal shock in the case of the CFTN tests and $MoSi_2$ altogether.

Chapter 5: Conclusion and Recommendations

It is concluded from the damage results that the $MoSi_2$ specimen becomes less brittle as the test temperatures increase. The particle velocities also seem to vary more in the CFTN than in the VHTN. The vitiated heating tests also prove that there are no signs of thermal shock at higher temperatures. The method of using the CFTN to impact the specimen is sufficient for this material at higher temperatures. The test setup presented both in the hot and cold fire tests prove simple and useful as the lack of accuracy was a non factor throughout the experiment. The ability to test several specimens in a short amount of time was achievable as opposed to the test setup shown in Appendix F.

5.1 Recommendations

Although the experiment proves as a useful method to perform impact tests, several design improvements exist to further advance this method of experimentation.

- The use of actuated valves to better maintain an increased exit temperature of the VHTN.
- Incorporate the use of a pyrometer or infrared laser to examine the characteristics at higher temperatures when utilizing the induction furnace.
- Examine a broad range of pressure ratios when dealing with the oxidizer and fuel and possibly utilize different fuels such as hydrogen.

References

[1] Byun, Thak S, Kim Jin, W, and Hong, Jun H. "A Theoretical Model for Determination of Fracture Toughness of reactor pressure Vessel Steels in the Transition Region from Automated Ball Indention Test" Journal of Nuclear Materials 252 (1998): 187-194.

[2] Abu-Farha, Fadi K. and Khraisheh, Marwan K. "On the High Temperature Testing of Superplastic Materials" Journal of Materials and Performance 16 (2007): 142-149.

[3] Mitani, Tohru. "Ignition Problems in Scramjet Testing" Combustion and Flame 101 (1995): 347-359).

[4] Hashimoto, T. "Combustion Stability of a Vitiated-Air Heater Using Coaxial Injectors" Energy Convers. Mgmt 38 (1997): 1083-1092.

[5] Andersson, Peter. "Water-Lubricated and Dry-Running Properties of Ceramic Journal Bearings" Tribotest Journal 10-2 (2003): 149-161.

[6] Belingardi, Giovannia and Vadori, Roberto. "Low Velocity Impact Tests of Laminate Glass-Fiber-Epoxy Matrix Composite Material Plates" International Journal of Impact Engineering 27 (2002): 213-229.

[7] Pogosyan, A.S. and Badyan, A. Kh. "Molybdenum Disilicide Heating Elements Manufactured by the High-Temperature Heating-Element Factory of Kirovakan" Powder Metallurgy and Metal Ceramics 9-12 (1970): 1023-1029.

[8] Mark, J.E. "Ceramic-Reinforced Polymers and Polymer-Modified Ceramics" Polymer Engineering and Science 36-24 (1996): 2905-2920.

[9] Bubnovich, V., Toledo, M., Gonzalez, H., and Salas R. "Finite Difference Study of Ignition in Methane-Air Mixture Flow" International Journal of Solids and Structures 40 (2003): 4955-4663.

[10] Tsigler, V. D. and Stovbur, A. V. "High-Alumina Insulation from Kyanite-Sillimanite Concentrate" Refactories and Industrial Ceramics 9 (1968): 435-455.

[11] Farooqi, J.K. and Sheikh, M.A. "Finite Element Modelling of Thermal Transport in Ceramic Matrix Composites" Computational Materials Sciences 37 (2006): 361-373.

[12] Lukin, E. S., Tarasova, S. V., and Korolev, A. V. "Appliction of Cermics Based on Aluminum Oxide In Medicine (Review)" Glass and Ceramics 58 (2001): 28-30.

[13] Schneider, H., Schreuer J., and Hildmann B. "Structure and Properties of Mullite-A Review" Journal of the European Ceramic Society 28 (2008): 329-344.

[14] Warnatz, J., Maas, U., and Dibble, R. W. Combustion: Physical and Chemical Fundamentals, Modeling and Simulation, Experiments, Pollutant Formation 4th ed. New York: Springer (1996): 145-148.

[15] Askeland, Donald R. and Phule, Pradeep P. The Science and Egnineering of Materials 4th ed. California: Brooks/Cole (2003): 261-262, 267.

Appendix A: Exit Temperature Plots of the CFTN

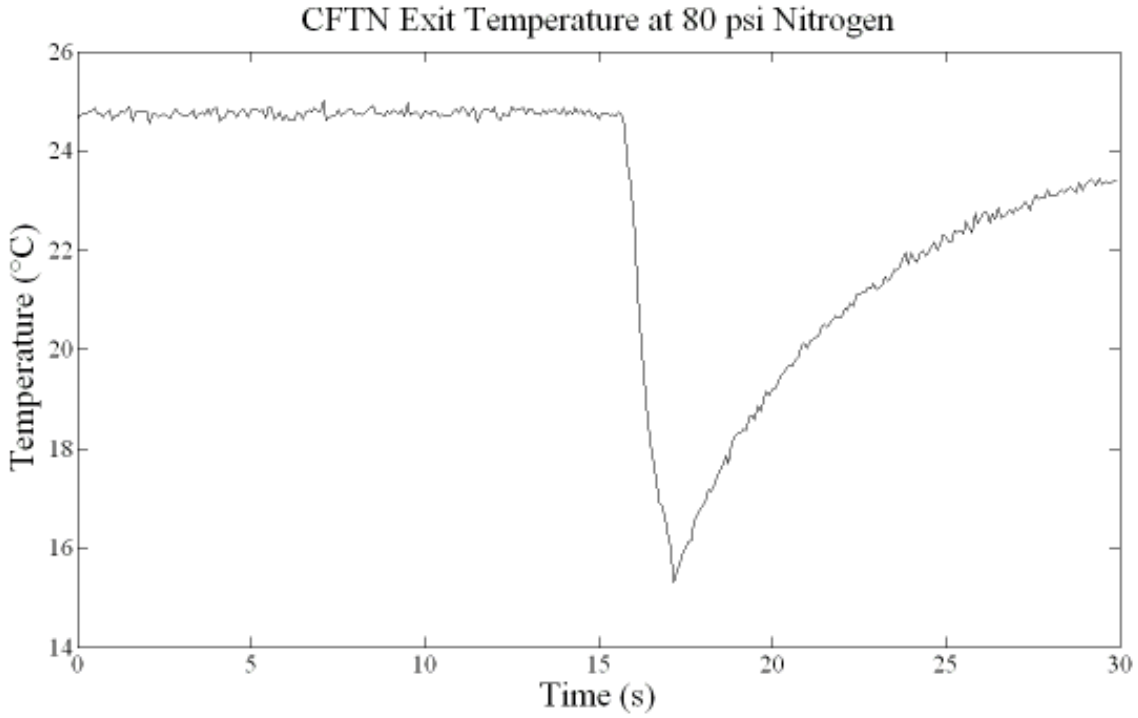

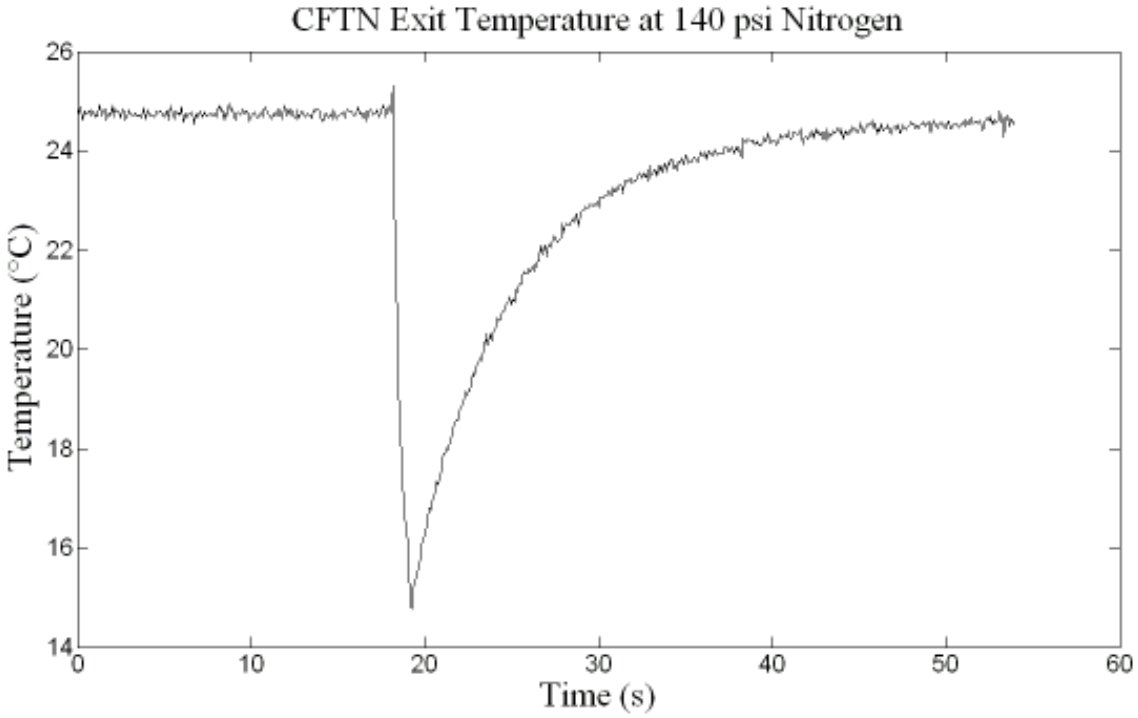

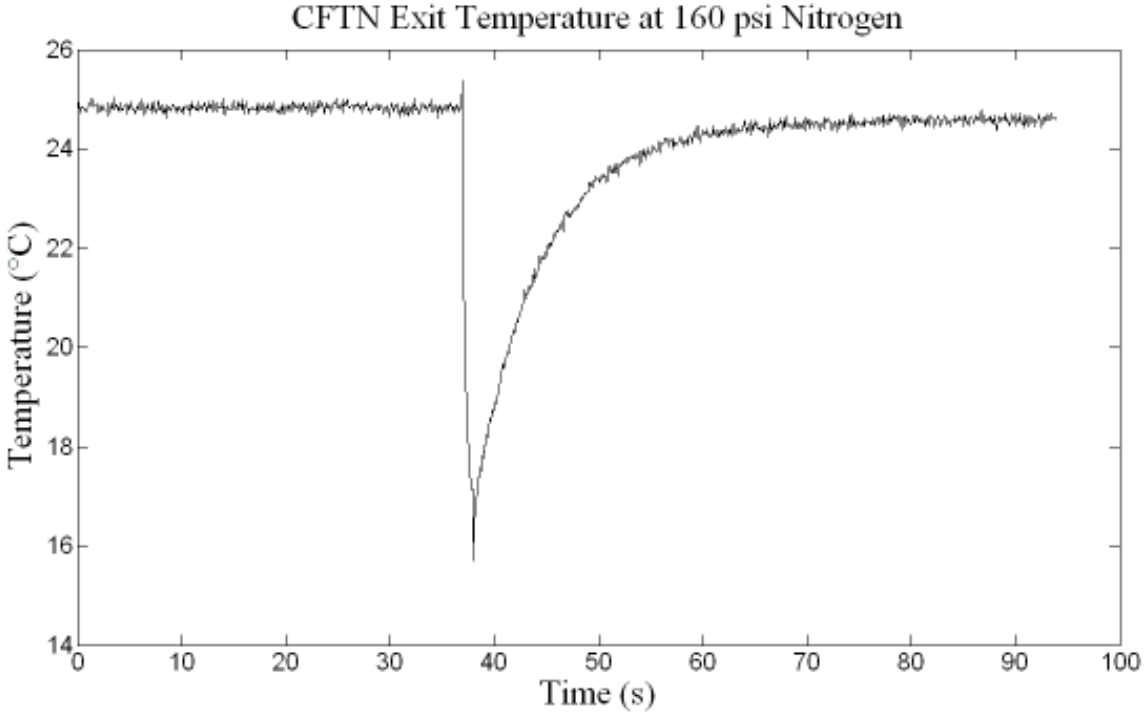
CFTN Exit Temperature at 160 psi Nitrogen
Temperature (°C)
Time (s)
26
24
22
20
18
16
14
0
10
20
30
40
50
60
70
80
90
100

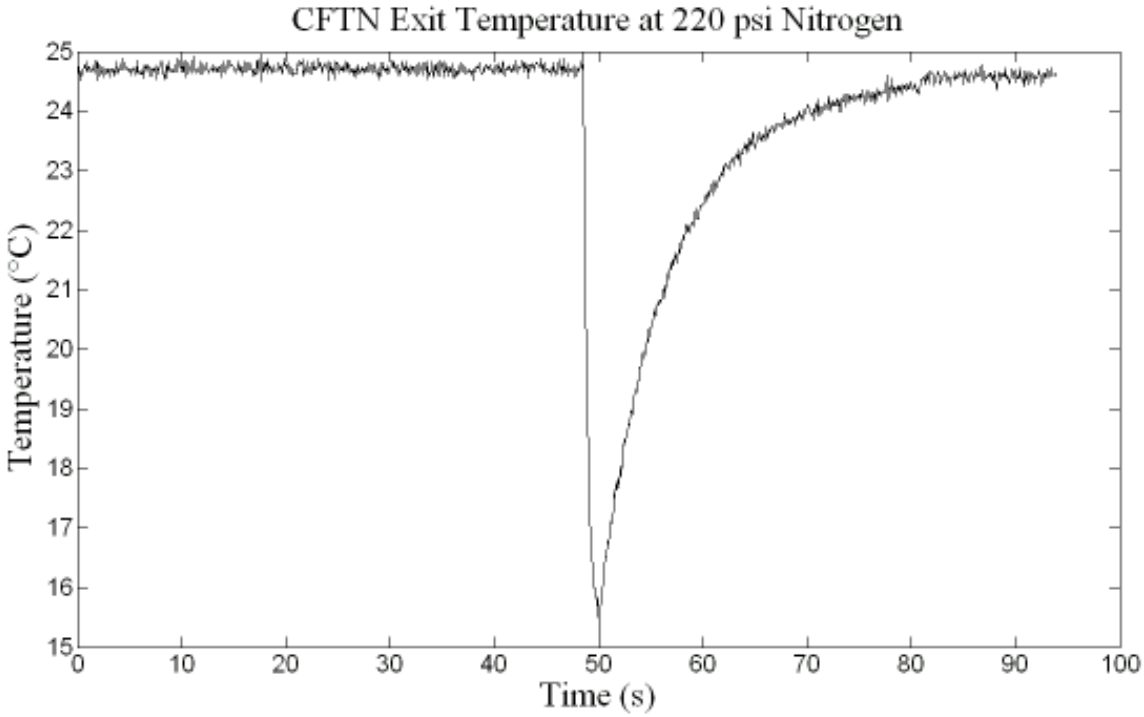
CFTN Exit Temperature at 220 psi Nitrogen
Temperature (°C)
Time (s)
25
24
23
22
21
20
19
18
17
16
15
0
10
20
30
40
50
60
70
80
90
100

Appendix B: Exit Temperature Plots of the VHTN

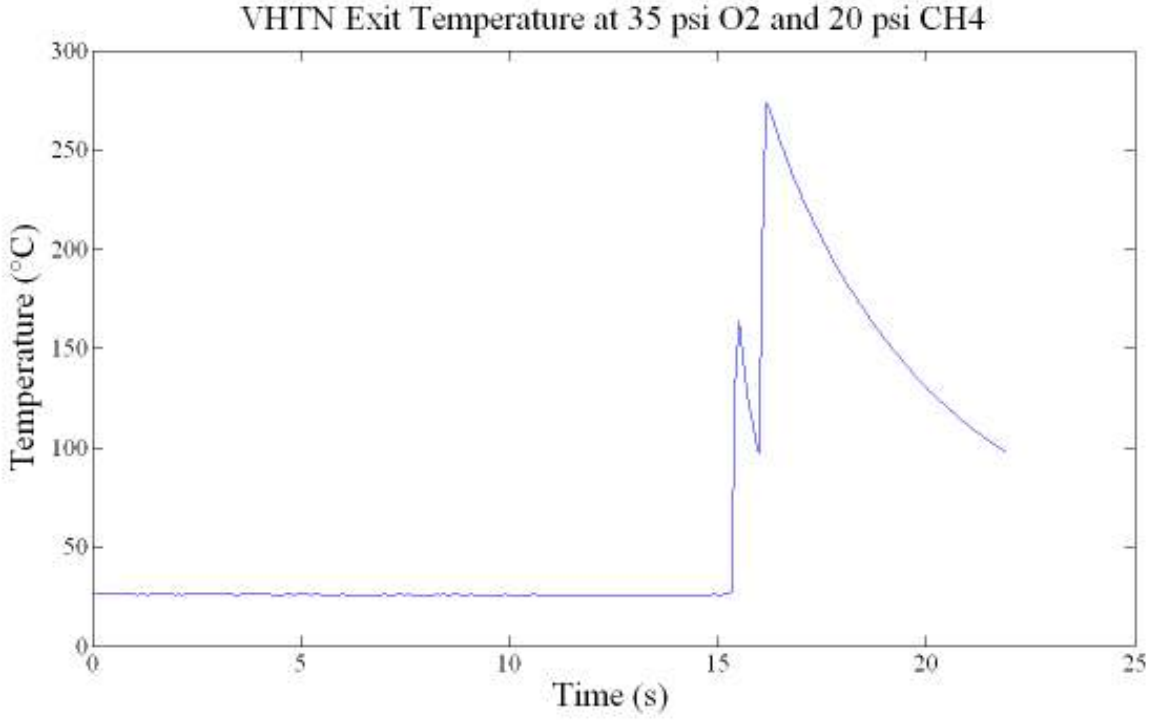

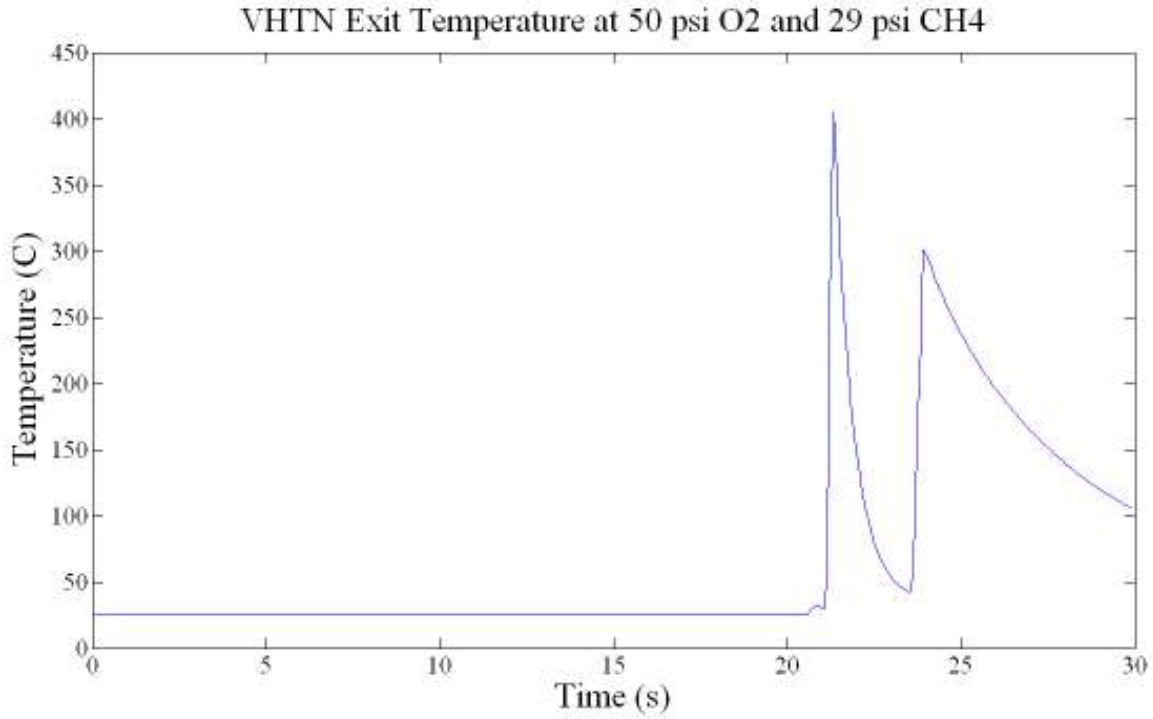

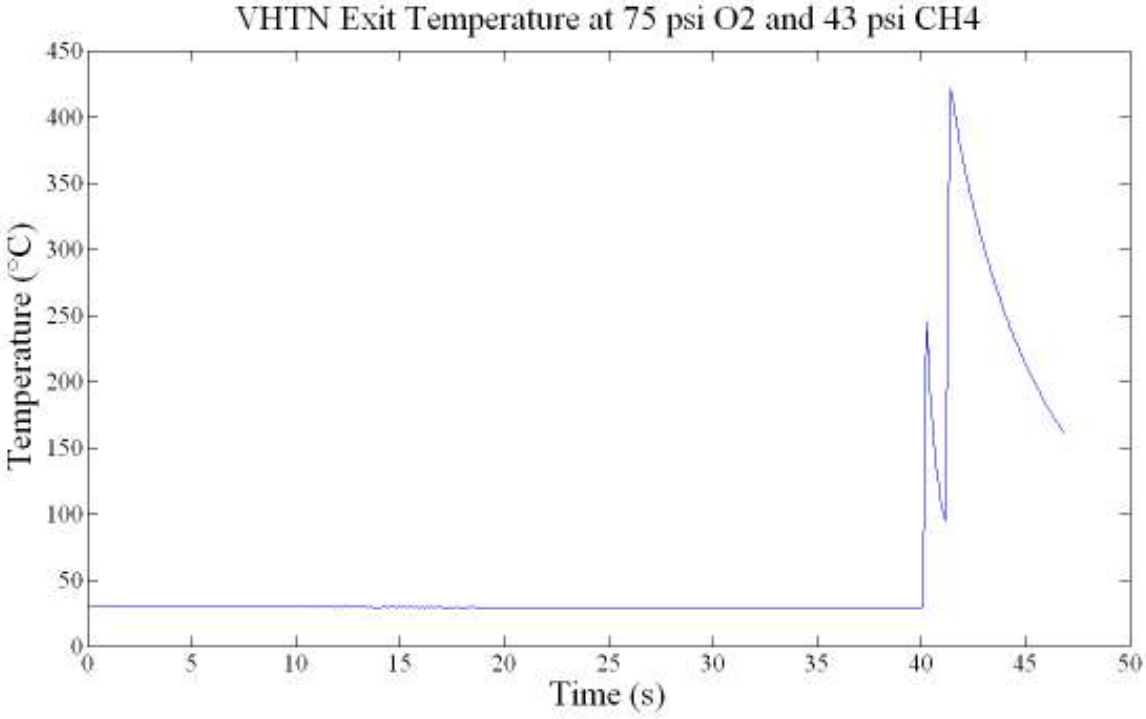
VHTN Exit Temperature at 75 psi O2 and 43 psi CH4
Temperature (°C)
Time (s)
0
50
100
150
200
250
300
350
400
450
0
5
10
15
20
25
30
35
40
45
50

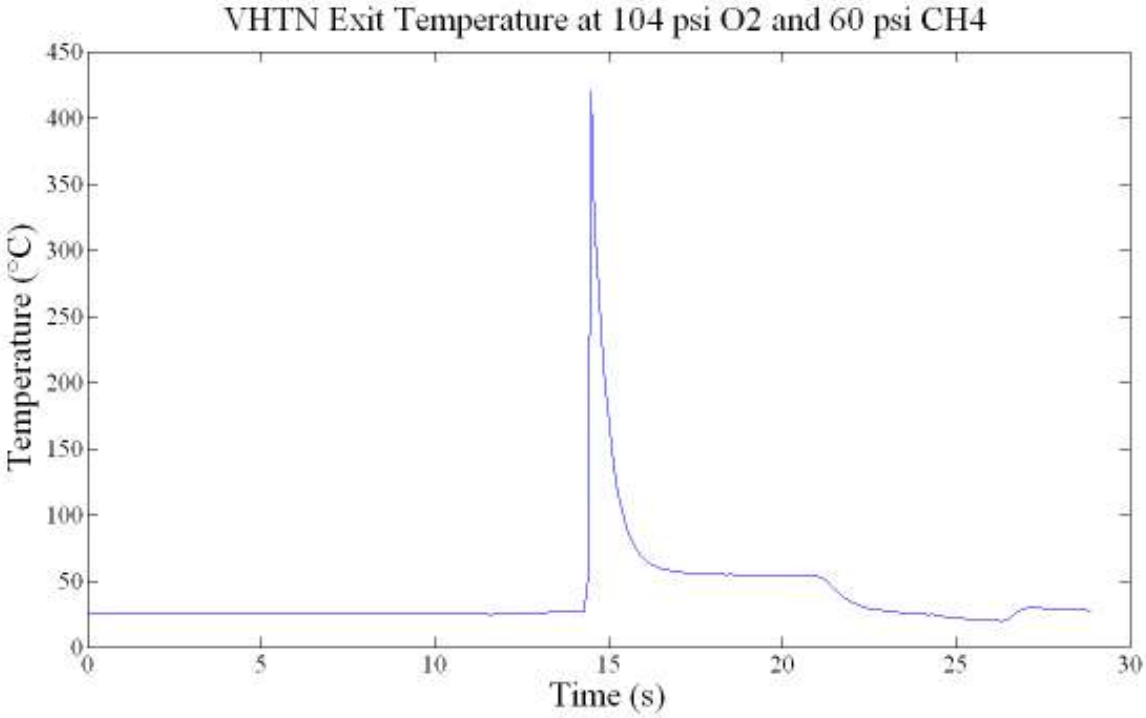
VHTN Exit Temperature at 104 psi O2 and 60 psi CH4
Temperature (°C)
Time (s)
0
50
100
150
200
250
300
350
400
450
0
5
10
15
20
25
30

Appendix C: Specimen Cracks (400 °C)

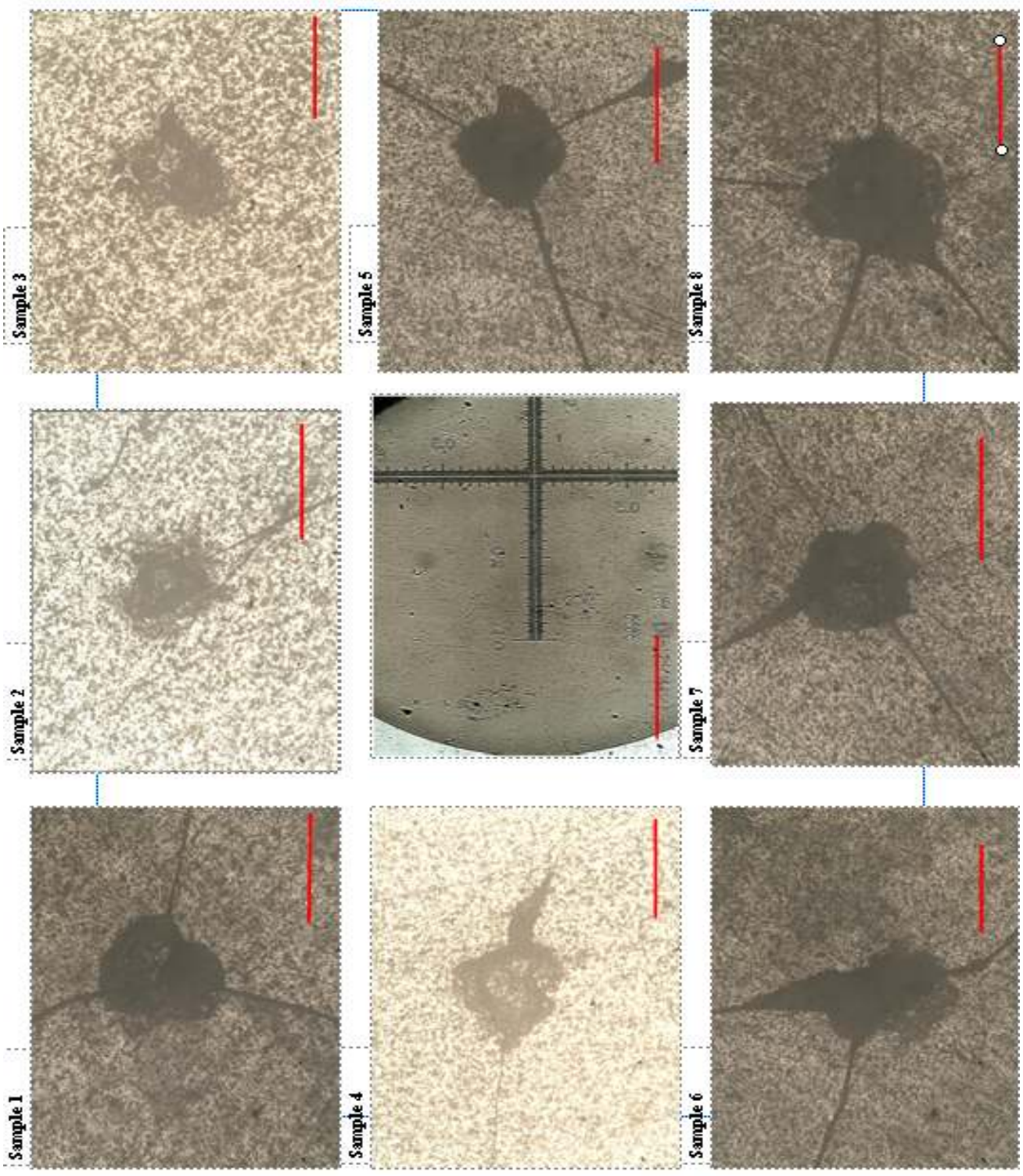

Sample 11
Sample 13
Sample 10
Sample 15
Sample 9
Sample 12
Sample 14

Appendix D: Specimen Cracks (1000 °C)

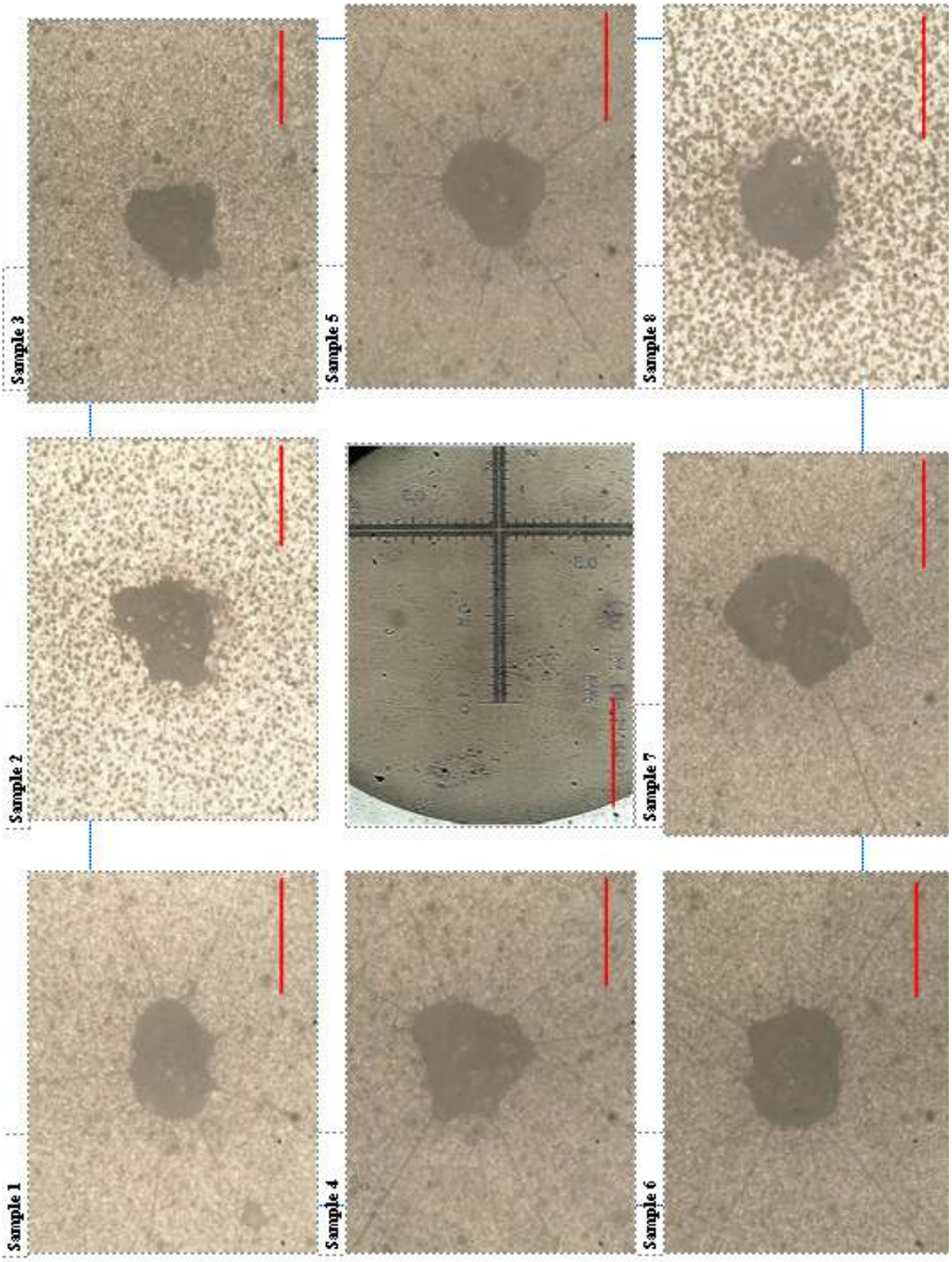

Sample 11
Sample 13
Sample 10
Sample 15
Sample 9
Sample 12
Sample 14

Appendix E: Specimen Cracks with VHTN Impact (1000°)

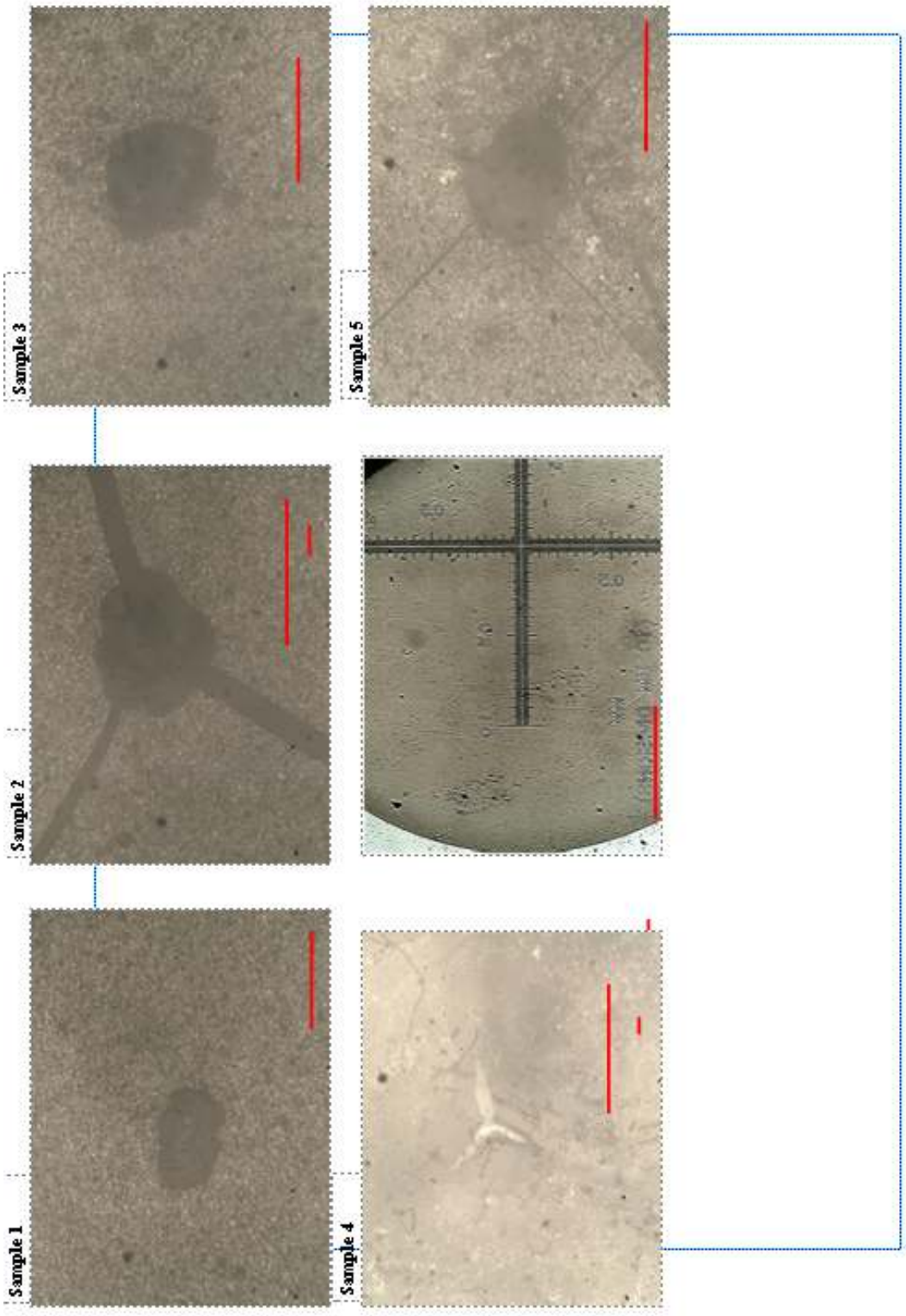

Appendix F: Previous Test Setups and Designs

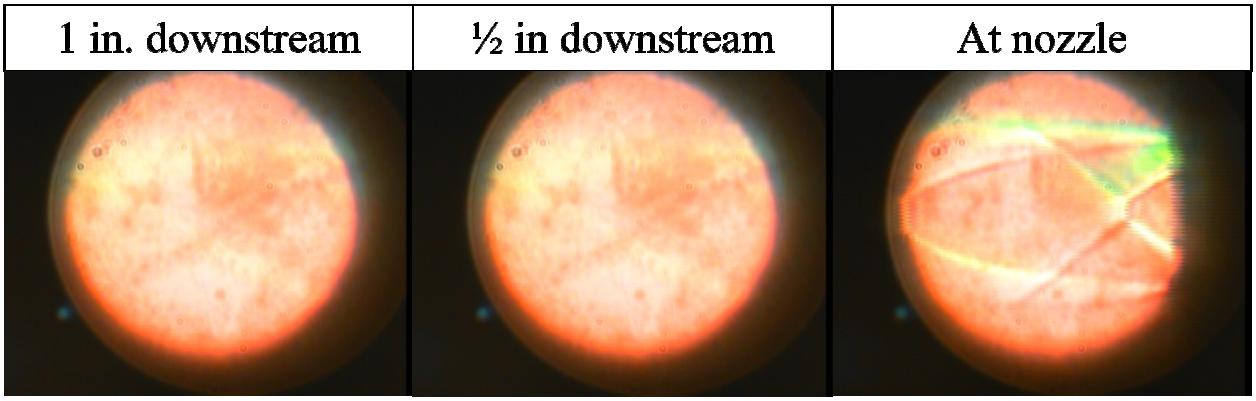

The Use of Schlieren Images to Examine the Downstream Flow of the CFTN

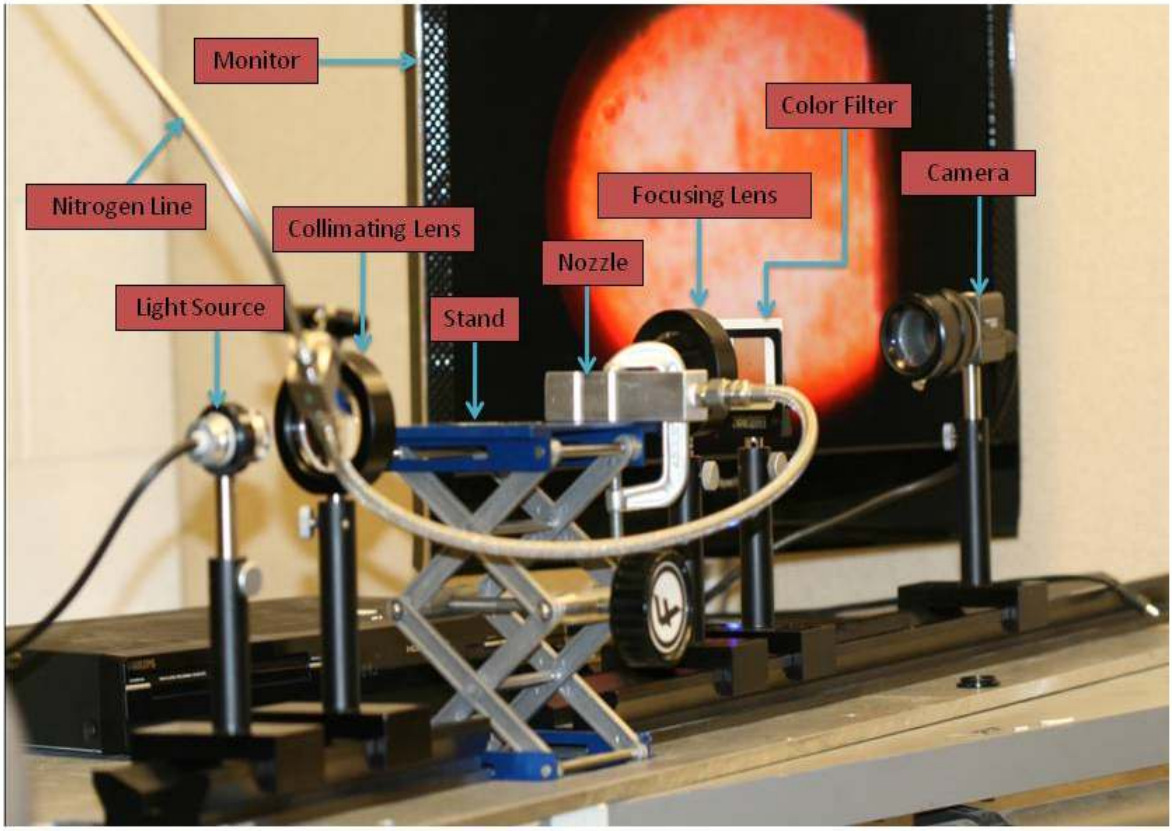

Schlieren System Setup

First Test Setup Utilizing the CM High Temperature Furnace

Mounting Stand and CFTN Nozzle During an Experiment with the High Temperature Furnace

Vita

Adrian Trejo was born July 31, 1984, in El Paso, Texas. Adrian graduated with a high school degree from Eastwood High School and attended The University of Texas at El Paso (UTEP) shortly after in the fall of 2002. During his time as an undergraduate student, he participated in activities such as Destination Imagination, Solar Car Project, and the Aerodesign Competition. In May of 2007 he received his Bachelor of Science degree in mechanical engineering and continued with his education at UTEP under the supervision of Dr. Thompson Sarkodi-Gyan. During his study as a graduate student, he published a journal titled "Mechanical Design of an Automated Gait Rehabilitation Machine" presented in the 24th Southern Biomedical Engineering Conference. He also attended the 1st Annual Texas Tech Research Colloquium presenting Neurorehabilitation for Human Subjects in a Zero Gravity Environment. Adrian is currently doing research under Dr. Jack Chessa investigating the impact on high temperature ceramics.

Permanent address: 10169 Honolulu
El Paso, Texas, 79925

This thesis/dissertation was typed by Adrian Trejo.